4 Polysaccharide-Based Composite Hydrogels for Removal of Pollutants from Water

Junping Zhang and Aiqin Wang

CONTENTS

4.1 INTRODUCTION

Hydrogels are cross-linked macromolecules with a 3D network that can entrap substantial amount of aqueous fluids. Due to the excellent properties compared to traditional water-absorbing materials, hydrogels have received much attention and are widely used in many fields, such as superabsorbents, tissue engineering, and pollutant adsorption (Lutolf and Hubbell 2005).

Hydrogels can be prepared using synthetic polymers, polysaccharides, and the mixture of them via covalent or noncovalent cross-linking. The absorption capacity and rate of hydrogels for aqueous fluids are determined by many factors including the nature of polymer precursors, the kind of hydrophilic groups, cross-linking degree, and surface morphology. Most of the hydrogels based on synthetic precursors,

for example, acrylic acid (AA), *N*-isopropylacrylamide (NIPAm), and acrylamide (AM), have excellent properties but are poor in degradability and biocompatibility. The potential of polysaccharides for the preparation of hydrogels has been widely recognized. Polysaccharides can easily form hydrogels by hydrogen bonding, ionic interactions, or chemical cross-linking. Incorporation of natural polysaccharides, such as starch and chitosan (CTS), can not only improve properties of corresponding hydrogels but also reduce our dependence on petrochemical-derived monomers. Sun et al. reported the synthesis of hydrogels from alginate and polyacrylamide (PAM) forming ionically and covalently cross-linked networks (Figure 4.1) (Sun et al. 2012). Although such gels contain 90% water, they can be stretched beyond 20 times their initial length and have fracture energies of 9000 J/m^2.

Polymer/layered silicate nanocomposites have attracted great interest because they often exhibit improved properties compared with virgin polymer or conventional micro- and macrocomposites (Ray and Okamoto 2003). These improvements include increased strength and heat resistance and decreased gas permeability and flammability. Most of the polymer/layered silicate nanocomposites are based on vinyl polymers (e.g., methyl methacrylate, acrylonitrile and styrene [St]), polycondensates (e.g., N6, poly(ε-caprolactone), and PDMS), polyolefins (e.g., polypropylene and polyethylene), and biodegradable polymers (e.g., poly(butylene succinate), unsaturated polyester, and polyhydroxy butyrate).

The commonly used clays for the preparation of nanocomposites are layered silicates. The layer thickness is around 1 nm, and the lateral dimensions of the layers vary from 30 nm to several microns, depending on the particular layered silicate. The layered silicates are characterized by moderate surface charge and specific surface area, which make them ideal materials for the reinforcement of polymers and adsorption of pollutants.

Traditional hydrogels from synthetic polymers often have some limitations besides poor biodegradability, which restrict their practical applications. Recently, biopolymer/inorganic material composites attracted much attention owing to their unique properties. Inorganic materials including clays, hydroxyapatite (HA), silica, and carbon nanotubes have been used for preparing this class of composites. The synergistic effect of biopolymer and inorganic material could improve the mechanical properties, swelling behavior, and other properties. In addition, these properties could be further tailored by altering the type and content of inorganic materials. Similarly, clay-based composite hydrogels are a type of very important hydrogels owing to the abundance of clay in nature and its low cost (Dawson et al. 2011). Clays, including montmorillonite (MMT), kaolin, and attapulgite (APT), have already been incorporated into traditional polymeric hydrogels, and encouraging results were obtained. For example, Wang et al. prepared a hydrogel by mixing water, Laponite XLG, a dendritic macromolecule, and sodium polyacrylate (Figure 4.2) (Wang et al. 2010d). This material can be molded into shape-persistent, free-standing objects owing to its exceptionally great mechanical strength and rapidly and completely self-heal.

Polysaccharide-based composite hydrogels are a new group of materials at the interface of hydrogels, polymer/clay nanocomposites, and polysaccharides. In this chapter, we reviewed the recent progress about this type of hydrogel. We discuss the preparation and characterization of the composite hydrogels, with an emphasis on

FIGURE 4.1 Schematics of three types of hydrogels. (a) In an alginate gel, the G blocks on different polymer chains form ionic cross-links through Ca^{2+} (circles). (*continued*)

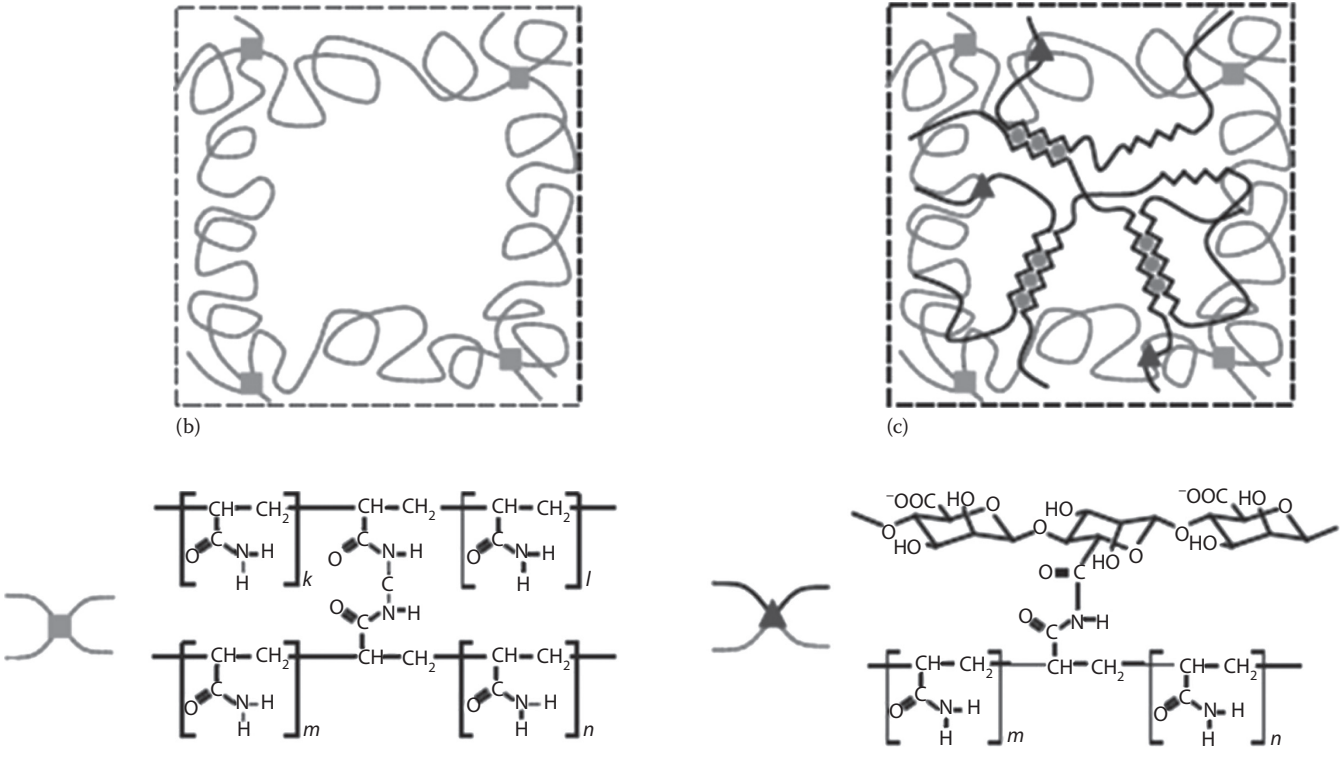

FIGURE 4.1 (continued) Schematics of three types of hydrogels. (b) In a PAM gel, the polymer chains form covalent cross-links through *N,N*-methylenebisacrylamide (MBA, squares). (c) In an alginate–PAM hybrid gel, the two types of polymer networks are intertwined and joined by covalent cross-links (triangles) between amine groups on PAM chains and carboxyl groups on alginate chains. (Reprinted with permission from Macmillan Publishers Ltd., *Nature*, Sun, J.Y., Zhao, X., Illeperuma, W.R., Chaudhuri, O., Oh, K.H., Mooney, D.J., Vlassak, J.J., and Suo, Z., 489, 133, Copyright 2012.)

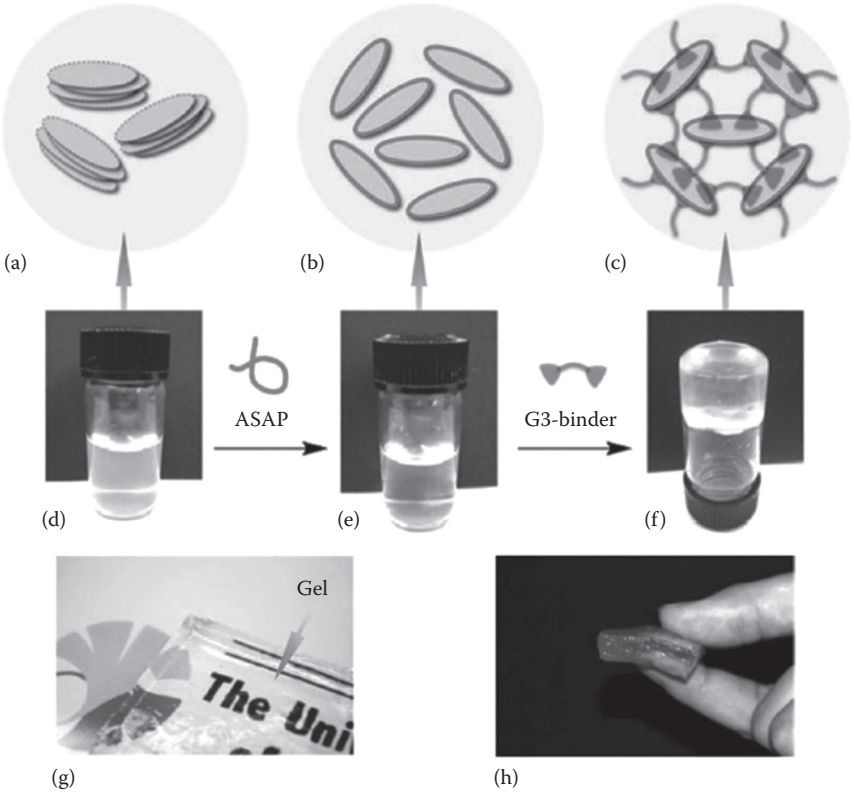

FIGURE 4.2 Noncovalent preparation of hydrogels. (a–c) Proposed mechanism for hydrogelation. CNSs, entangled with one another (a), are dispersed homogeneously by interaction of their positive-charged edge parts with anionic ASAP (b). Upon addition of Gn-binder, exfoliated CNSs are crosslinked to develop a 3D network (c). (d–f) Optical images of an aqueous suspension of CNSs (d), an aqueous dispersion of CNSs and ASAP (e), and a physical gel upon addition of G3-binder to the dispersion (f). (g, h) The gel is transparent (g) and free standing (h). (From Wang, Q.G. et al., Nature, 463, 339, 2010b. With permission.)

structure and swelling properties. Moreover, we summarized the applications of the composite hydrogels for the removal of pollutants including heavy metals, dyes, and ammonium nitrogen from water.

4.2 POLYSACCHARIDE-BASED COMPOSITE HYDROGELS

4.2.1 Chitosan-Based Composite Hydrogels

CTS is the most abundant biomass in the world. It is made by treating shrimp and other crustacean shells with sodium hydroxide. CTS is a linear polysaccharide composed of randomly distributed β-(1–4)-linked D-glucosamine and *N*-acetyl-D-glucosamine.

Most of the applications of CTS are based on the polyelectrolytic nature and chelating ability of the amine group. The positively charged CTS could interact with the negatively charged layers of many clay minerals, which results in the intercalation

or exfoliation of clays. Ruiz-Hitzky et al. reported a CTS/Na–MMT nanocomposite that can be combined with graphite to construct bulk-modified electrodes, which show high selectivity toward monovalent anions (Margarita et al. 2003). They also prepared CTS/sepiolite (SP) nanocomposites and proposed the interaction mechanism between them (Margarita et al. 2006). Due to the strong interaction between CTS and SP, the mechanical properties were evidently improved with respect to the virgin polymer. In addition, the reactive $–NH_2$ and –OH groups of CTS are convenient for its reaction with other polymers or monomers (e.g., carboxymethyl cellulose [CMC], *N*-vinylpyrrolidone, and AA) (Shang et al. 2008). CTS has been widely used in fabricating biomedical hydrogels owing to its biocompatibility and antibacterial properties. Inspired by the excellent properties of CTS/clay nanocomposites and CTS-based hydrogels, various composite hydrogels based on CTS and clays were reported. APT is a crystalline hydrated magnesium silicate with a fibrous morphology, which is composed of talc-like units arranged alternately, generating tunnels of 3.7 Å × 6.4 Å along the *c*-axis of the fiber (Figure 4.3) (Bradley 1940).

APT has large specific surface area, moderate cation exchange capacity, and reactive –OH groups on its surface, which makes it an excellent material for the preparation of polymer/clay nanocomposites (Neaman and Singer 2004). Wang et al. prepared the

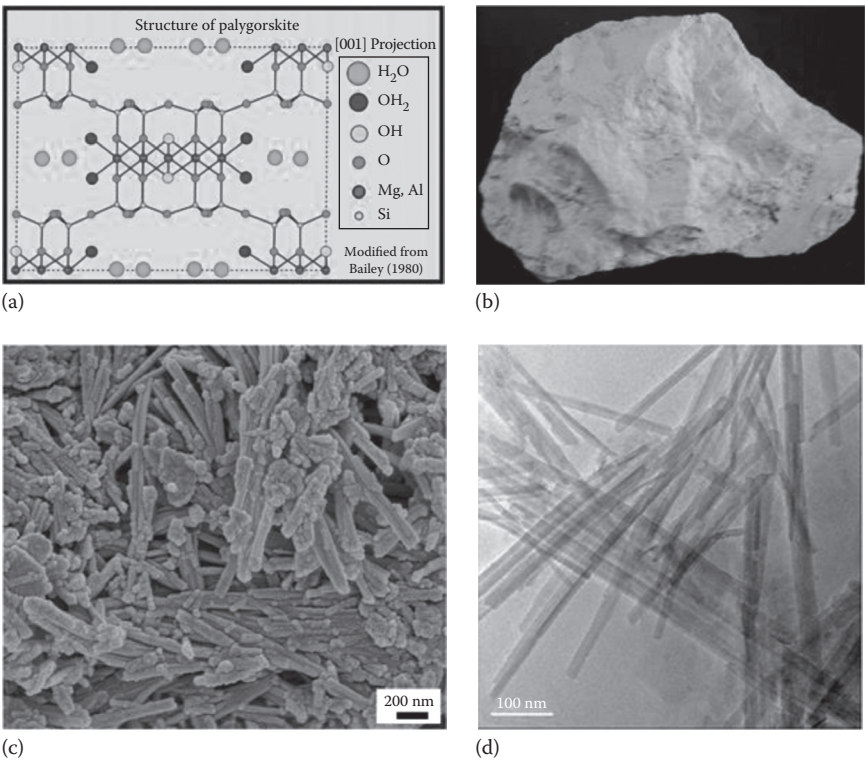

FIGURE 4.3 (a) Structure. (From http://pubs.usgs.gov/of/2001/of01-041/htmldocs/clays/seppaly.htm.) (b) Digital. (c) SEM. (d) TEM images of APT.

CTS/APT composite microspheres via spray-drying (Wang et al. 2011c). The introduction of APT can not only enhance the isoelectric points but also achieve narrow size distribution of the microspheres. A series of ofloxacin/MMT/CTS (OFL/MMT/CTS) composite hydrogels were prepared by solution intercalation and ionic cross-linking with sodium tripolyphosphate (TPP) (Hua et al. 2010). The electrostatic interaction between CTS and MMT enhanced the stability and swelling behavior of the beads. Hua et al. designed pH-sensitive OFL/MMT/CTS nanocomposite microspheres by the solution intercalation and emulsification cross-linking techniques (Hua et al. 2008). Yang et al. developed a series of CTS/Laponite composite beads by using TPP as the ionic cross-linker (Yang et al. 2011). The exfoliated sheets of Laponite act as physical cross-linkers to facilitate the formation of network structure between CTS and Laponite.

We have prepared for the first time the CTS-*g*-poly(acrylic acid)/APT (CTS-*g*-PAA/APT) composite hydrogels (Figure 4.4) (Zhang et al. 2007b). The –OH of APT and –OH and $–NH_2$ of CTS participated in graft polymerization with AA. In addition, the introduced APT could enhance thermal stability and form a porous surface. By Ca^{2+} cross-linking of the CTS-*g*-PAA/APT composite hydrogel with sodium alginate (SA), Wang et al. obtained novel pH-sensitive composite hydrogel beads (Wang et al. 2009a). Moreover, the CTS-*g*-PAA/APT composite hydrogel can be easily scaled up. This composite hydrogel has been proved to be an excellent material for the removal of ammonium nitrogen (NH_4^+-N) (Zheng et al. 2009b), methylene blue (MB) (Wang et al. 2011b), and heavy metals (Wang and Wang 2010b, Wang et al. 2009g) from aqueous solution.

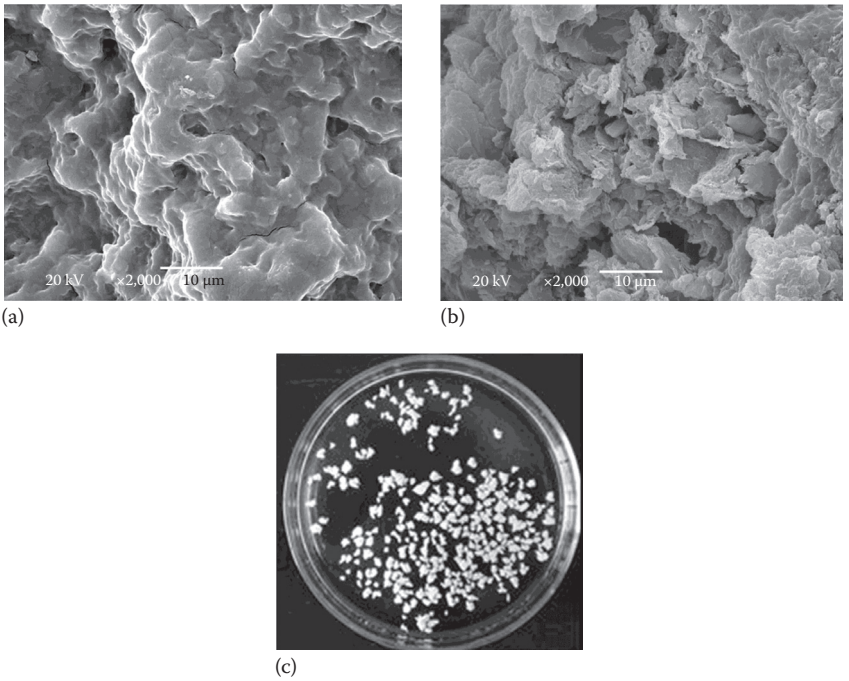

FIGURE 4.4 SEM micrographs of (a) CTS-*g*-PAA and (b) CTS-*g*-PAA/APT composite hydrogels. (c) Image of the granular composite hydrogel.

Liu et al. have studied the effect of grinding of APT on swelling properties of the CTS-*g*-PAA/APT nanocomposite hydrogels (Liu et al. 2013b). Grinding could decrease the length of single crystals and dissociate part of crystal aggregates of APT, which affect the dispersion of APT in the polymeric matrix, thus leading to change in swelling behaviors of the nanocomposites.

We also introduced MMT into the CTS-*g*-PAA hydrogel (Figure 4.5) (Zhang et al. 2007a). CTS could intercalate into the layers of MMT and form nanocomposites

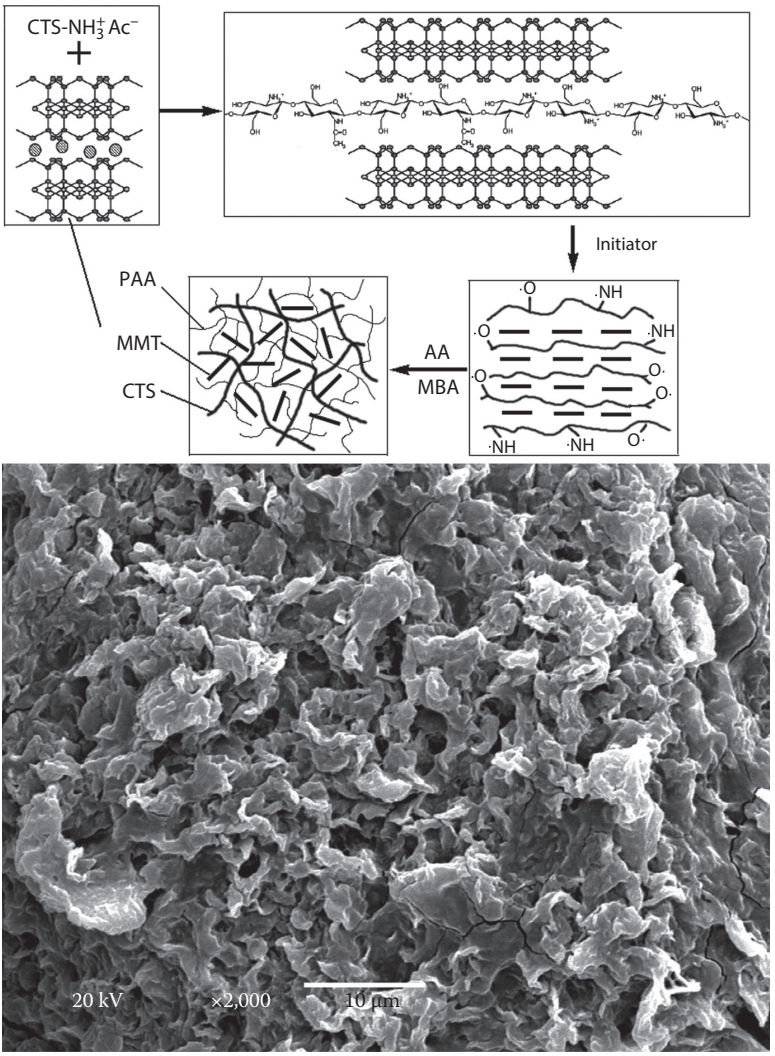

FIGURE 4.5 Schematic representation of the CTS-*g*-PAA/MMT nanocomposite hydrogel prepared via in situ polymerization and the corresponding SEM image. (Reprinted with permission from Zhang, J.P., Wang, L., and Wang, A.Q., *Ind. Eng. Chem. Res.*, 46, 2497. Copyright 2007 American Chemical Society.)

through in situ graft polymerization with AA. The surface morphology of the CTS-*g*-PAA/MMT nanocomposite is different from that of CTS-*g*-PAA. Compared to the tight surface of CTS-*g*-PAA, the surface of the CTS-*g*-PAA/MMT nanocomposite is more loose and porous, which is convenient for the penetration of water into the polymeric network and is of benefit to improve the water absorbency.

Owing to the excellent properties of CTS-based composite hydrogels, we also prepared many composite hydrogels using other clays instead of APT and MMT. Clays including rectorite (REC) (Liu and Wang 2008a,b, Zheng and Wang 2009), vermiculite (VMT) (Xie and Wang 2009a,c), SP (Xie and Wang 2009b, Xie et al. 2010), and halloysite nanotubes (HNTs) (Zheng and Wang 2010c) were used. These clays are different in crystalline structure, morphology, and properties.

REC is a kind of layered silicate with structure and characteristics like bentonite. The introduction of REC into the polymer matrix can not only improve the thermal stability of the corresponding polymer but also reduce the product cost. A series of nanocomposites based on REC, CTS, and its derivatives has been reported (Huang et al. 2012b, Li et al. 2011b, Liu et al. 2012a, 2013a, Wang et al. 2007, 2010g,h, Xu et al. 2012). CTS/organic rectorite (CTS/OREC) nanocomposite films were obtained by a casting/solvent evaporation method. The addition of OREC to pure CTS film influenced many of the properties. Liu et al. reported the preparation of the exfoliated quaternized carboxymethyl CTS/REC (QCMC/REC) nanocomposite via microwave irradiation method, which was performed in only water without any additional plasticizer (Liu et al. 2012a). Two types of interactions of hydrogen bond and electrostatic attraction exist in the QCMC/REC nanocomposite. Liu and Wang prepared the CTS-*g*-PAA/REC composite hydrogels through graft polymerization among REC, CTS, and AA in aqueous solution (Liu and Wang 2008a). They also studied the effect of modification of REC with hexadecyltrimethylammonium bromide (HDTMABr) on properties of the composite hydrogel (Liu and Wang 2008b). CTS-*g*-PAA/OREC nanocomposites show an exfoliated nanostructure. The water absorbency of CTS-*g*-PAA/OREC increased with increasing organification degree of OREC owing to the improved compatibility of polymer matrix and OREC.

VMT is a layered aluminum silicate with exchangeable cations and reactive –OH groups on the surface (Zheng et al. 2007). The CTS/VMT nanocomposites were prepared by the solution mixing process of CTS with three different modified VMTs (HVMT, NVMT, and organo-VMT [OVMT]), which were treated by HCl, NaCl, and HDTMABr, respectively (Zhang et al. 2009). The modification and the nanoscale dispersion of the modified VMTs were confirmed by x-ray diffraction (XRD) and TEM. The thermal stability of CTS/HVMT, CTS/NVMT, and CTS/OVMT nanocomposites were significantly improved compared to that of neat CTS. Introducing HVMT into CTS matrix can enhance the thermal stability due to the well dispersion of HVMT and better interaction between HVMT and CTS. VMT also can improve water absorbency of the composites (Zheng et al. 2007).

The CTS-*g*-PAA/unexpanded VMT (CTS-*g*-PAA/UVMT) composite hydrogels were prepared by graft polymerization (Xie and Wang 2009c). The reactions between AA and –OH groups of UVMT could improve the polymeric network and then enhance the water absorbency. They also studied the effects of acid-activated, ion-exchanged, and organic-modified VMT on properties of the CTS-*g*-PAA/VMT composite

hydrogels (Xie and Wang 2009c). The modification of VMT could improve water absorbency and swelling rate. By dispersing microparticles of the CTS-*g*-PAA/VMT composite hydrogel into SA aqueous solution and then cross-linked with Ca^{2+}, Wang et al. prepared pH-sensitive composite hydrogel beads (Wang et al. 2010b).

SP is a hydrated magnesium silicate clay mineral with microfibrous morphology. A significant number of silanol groups are present at the surface of these minerals, and these groups are directly accessible to various reagents (Tekin et al. 2006). Huang et al. prepared the CTS/PVA nanocomposite films reinforced with SP (Huang et al. 2012a). The mechanical properties were improved with an increase in SP loading, but the moisture uptake decreased.

A CTS-*g*-PAA/SP composite hydrogel was prepared by graft polymerization among CTS, AA, and SP. CTS and SP participated in graft polymerization with AA. The introduced SP enhanced swelling rate and water absorbency (Xie and Wang 2009b). In addition, the modification of SP (acid-activated SP and cation-exchanged SP) also has influenced the water absorbency and swelling behavior (Xie et al. 2010). Water absorbency and swelling behavior depend strongly on HCl concentration and the kinds of cation exchanged. The introduction of suitable amount of acid-activated and cation-exchanged SP could not only enhance water absorbency but also improve the swelling rate. Shi et al. found that SP could improve the adsorption rate, gel strength, and acid and salt resistance of the CTS-*g*-PAA/SP composite hydrogels (Shi et al. 2011a).

HNTs, a kind of aluminosilicate mineral, are chemically similar to kaolin, but morphologically have a hollow tubular structure. Due to special hollow tubular structure and excellent properties, HNTs have potential applications in many fields and have attracted considerable attention (Shchukin et al. 2008). Various CTS/HNT nanocomposites have been prepared. Deen et al. reported electrophoretic deposition of composite CTS–HNT–HA films (Figure 4.6) (Deen et al. 2012). The use of CTS as a dispersing and charging agent for both HNTs and HA allowed the formation of CTS–HNT–HA monolayers, which showed corrosion protection of the stainless steel substrates.

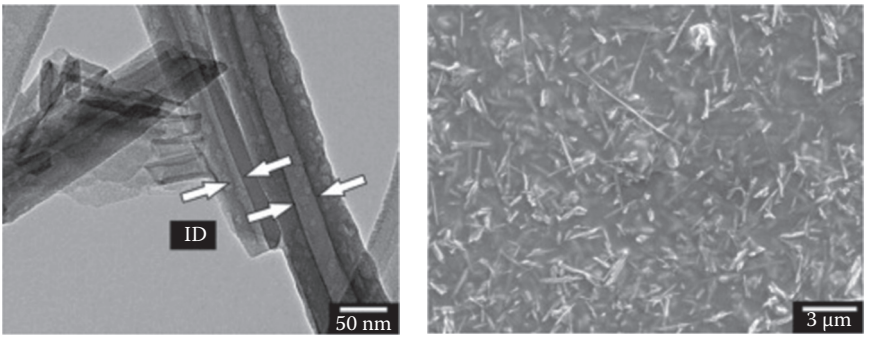

(a) (b)

FIGURE 4.6 (a) TEM and (b) SEM of the CTS–HNT–HA film. (Reprinted from *Colloids Surf. A*, 410, Deen, I., Pang, X., and Zhitomirsky, I., Electrophoretic deposition of composite chitosan–halloysite nanotube–hydroxyapatite films, 38–44, Copyright 2012, with permission from Elsevier.)

Zheng et al. grafted PAA onto CTS to form granular hydrogel composites with HNTs (Zheng and Wang 2010c). HNTs are in the form of partially hydrated state and no additional interaction is present among the reactants. The sample surface gets coarse and many micropores are visible by introducing HNTs into the hydrogel. Wang et al. prepared the CTS-*g*-PAA/HNT/SA composite hydrogel by the ionic gelation method (Wang et al. 2010c). The HNT content obviously influences the swelling ratio and cumulative release of diclofenac sodium (DS).

Muscovite (MVT, mica) is a tetrahedral–octahedral–tetrahedral-structured phyllosilicate (Klien et al. 2008). There are reactive –OH groups on the surface of MVT and these groups are accessible to prepare organic–inorganic nanocomposites (Xie and Wang 2010). Huang et al. reported an anti-UV CTS/mica copolymer (Huang et al. 2010). The modified mica distributes homogeneously on the surface of the copolymer films. Xie et al. introduced MVT during the free radical graft polymerization of CTS and AA and got granular composite hydrogels (Xie and Wang 2010). AA was grafted onto CTS and –OH groups of MVT participated in the reaction. Ion-exchanged MVT could improve water absorbency and swelling rate compared to the pristine MVT.

Sodium humate (SH) is composed of multifunctional aliphatic components and aromatic constituents. SH contains a large number of functional groups, for example, carboxylates and phenolic hydroxyls (Hayes et al. 1989). A series of superabsorbents based on SH was prepared considering that SH can regulate plant growth, accelerate root development, enhance photosynthesis, improve soil cluster structures, and enhance the absorption of nutrient elements (Zhang et al. 2005).

On the basis of SH-based superabsorbents, we introduced SH into the CTS-*g*-PAA system instead of clay minerals. Liu et al. reported a novel CTS-*g*-PAA/SH composite hydrogel via graft polymerization (Liu et al. 2007). CTS and SH participated in graft polymerization reaction with AA. The introduced SH could enhance water absorbency. APT and SH were also incorporated together into the CTS-*g*-PAA system (Zhang et al. 2011, Zhang and Wang 2010). The synergistic effect of APT and SH on swelling capacity was observed.

In spite of unique properties, CTS is only soluble in acidic solution, which hindered its applications. Chemical modification is a frequently used method to make it soluble in water. Various studies were conducted to make derivatives of CTS, such as PEG grafting, sulfonation, *N*- and *O*-hydroxylation, and carboxymethyl CTS (Wang et al. 2006). The derivatives of CTS were also used for preparing composite hydrogels. A novel *N*-succinylCTS-*g*-polyacrylamide/APT (NSC-*g*-PAM/APT) composite hydrogel was prepared by inverse suspension polymerization (Li et al. 2007b). –OH of APT and –OH and –NHCO of NSC participated in graft polymerization with AM. The introduced APT could enhance the thermal stability of the hydrogel. The composite hydrogel has a microporous surface and shows higher swelling rate compared to that of without APT. Ma et al. prepared pH- and temperature-responsive semi-interpenetrating polymer network (semi-IPN) hydrogels of carboxymethyl CTS with poly(*N*-isopropylacrylamide) (PNIPAm) crosslinked by Laponite XLG (Ma et al. 2007). The hydrogels exhibited a volume phase transition temperature (VPTT) around 33°C with no significant deviation from the conventional PNIPAm hydrogels.

4.2.2 Starch-Based Composite Hydrogels

Starch is among the most abundant and inexpensive biopolymers. Most starches are composed of two structurally distinct molecules: amylose, a linear or lightly branched (1 → 4)-linked α-glucopyranose, and amylopectin, a highly branched molecule of (1 → 4)-linked α-glucopyranose with α-(1 → 6) branch linkages.

Starch is one of the ideal biopolymers for the preparation of biopolymer/clay nanocomposites. Various clays (e.g., Laponite, kaolin, and MMT) and starches (e.g., cassava starch, cationic starch, and cornstarch) have been used for the preparation of starch-based nanocomposites. Chivrac et al. reported a new approach to elaborate exfoliated starch-based nanobiocomposites (Chivrac et al. 2008). They used cationic starch as a new clay organomodifier to better match the polarity of the matrix and thus to facilitate the clay exfoliation process.

In 2000, Wu et al. reported synthesis and properties of starch-*g*-PAM/clay composite hydrogels (Wu et al. 2000). Clays including bentonite and sercite are used for preparing the composite hydrogels. The kind of clay is an important factor affecting absorbent properties since the composite was formed by a reaction between –OH groups of clay and organic groups of starch and AM. In addition, the hydration of clay is also an important factor influencing the swelling capacity.

Li et al. prepared the starch-*g*-PAM/APT composite hydrogels via graft polymerization reaction (Li et al. 2005). The graft polymerization between –OH groups on APT and monomers took place during the reaction. The introduction of 5% APT could increase the water absorbency from 545 g/g of the neat starch-*g*-PAM to 1317 g/g (Li et al. 2004, Lin et al. 2001). Zhang et al. prepared the starch phosphate-*g*-PAM/APT composite hydrogels (Zhang et al. 2006). The composite hydrogel acquired the highest water absorbency of 1268 g/g when 10% APT was incorporated. The introduced starch phosphate and APT endowed the composite with a higher thermal stability, greatly improved water absorbency, and salt-resistant properties.

AA is also a frequently used monomer besides AM to prepare starch- or clay-based composite hydrogels. Li et al. synthesized the starch-*g*-PAA/APT composite hydrogels with a water absorbency of 1077 in distilled water (Li et al. 2007a). This composite hydrogel could be useful in agricultural and horticultural applications. Luo et al. prepared starch-*g*-P(AM-*co*-AA)/MMT nanosuperabsorbent via γ-ray irradiation (Luo et al. 2005). The layers of MMT are exfoliated and uniformly dispersed in the polymer matrix. Hua et al. prepared the starch-*g*-PAA/SH composite hydrogels (Hua and Wang 2008). SH can improve the swelling rate and reswelling capability.

4.2.3 Cellulose-Based Composite Hydrogels

Cellulose, the most abundant natural material, is a frequently used natural polymer for the preparation of nanocomposites. Various clays including MMT and Laponite have been used. Liu et al. reported a clay nanopaper with tough nanofibrillated cellulose matrix for fire retardancy and gas barrier functions, which is of interest in self-extinguishing composites and in oxygen barrier layers (Liu et al. 2011d). Perotti et al. reported bacterial cellulose/Laponite clay nanocomposites with greatly enhanced Young modulus and tensile strength (Perotti et al. 2011).

To prepare hydrogels, derivatives of cellulose soluble in aqueous phase are necessary, which is convenient for the graft polymerization of monomers onto the backbone. CMC is a representative cellulose derivative. It can be easily produced by the alkali-catalyzed reaction of cellulose with chloroacetic acid. The polar carboxyl groups render cellulose soluble in aqueous solution, chemically reactive, and hydrophilic (Wang and Wang 2010a). Li et al. prepared the CMC/MMT composite hydrogels for the controlled release of acetochlor (Li et al. 2008). The performance of inorganic clays on slowing the release of acetochlor is related to their sorption capacities. Wang et al. reported a nanocomposite hydrogel of CMC and APT by free radical polymerization of CMC, AA, and APT (Wang et al. 2010a). APT nanofibers were retained in nanocomposite and uniformly dispersed in the CMC-*g*-PAA matrix. The thermal stability and water absorption of the nanocomposites were improved by APT.

REC, medical stone (MS), and SH were also introduced into CMC-*g*-PAA instead of APT and promising results were obtained (Chen et al. 2010, Wang and Wang 2011, Wang et al. 2011f). REC was exfoliated and uniformly dispersed in the CMC-*g*-PAA matrix (Figure 4.7). The thermal stability and swelling capability were improved by introducing REC. The nanocomposite showed excellent responsive properties and reversible on–off switching characteristics in various saline, pH, and organic solvent/water solutions (Wang and Wang 2011). The incorporation of 20% MS evidently enhanced the water absorbency by 100% (Wang et al. 2011f). Chen et al. introduced APT and SH simultaneously into the CMC-*g*-PAA matrix (Chen et al. 2010). The composite hydrogel acquired the highest water absorbency of 582 g/g when 5% HA and 30% APT were introduced. Wang et al. prepared the CMC-*g*-PAA/APT/SA composite hydrogel beads by ionic cross-linking (Wang et al. 2012a). Introducing 20% APT into CMC-*g*-PAA

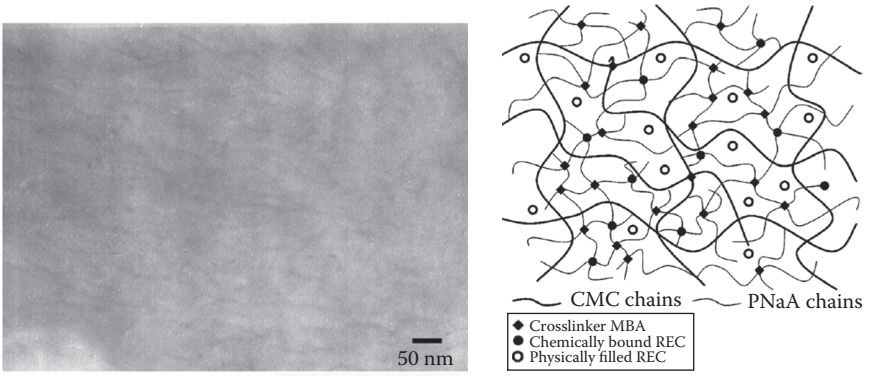

FIGURE 4.7 (a) TEM image of CMC-*g*-PAA/REC (5 wt% REC) composite hydrogel and (b) the schematic network structure. (Wang, W.B. and Wang, A.Q., Preparation, swelling, and stimuli-responsive characteristics of superabsorbent nanocomposites based on carboxymethyl cellulose and rectorite. *Polym. Adv. Technol.* 2011. 22. 1602–1611. Copyright Wiley-VCH Verlag GmbH & Co. KGaA. Reproduced with permission.)

hydrogel could change the surface structure of the composite hydrogel beads, decrease the swelling ability, and relieve the burst release of DS.

Ma et al. prepared a semi-IPN CMC/PNIPAm/clay nanocomposite hydrogel using Laponite XLG (Ma et al. 2008). The clay was substantially exfoliated to form nanodimension platelets dispersed homogeneously in the hydrogels and acted as a multifunctional cross-linker. Hydroxyethyl cellulose (HEC) is another representative derivative of cellulose with excellent water solubility and biocompatibility. Because of the existence of abundant reactive –OH groups, HEC is liable to be modified by grafting polymerization with vinyl monomers to derive new materials. APT, VMT, and MS have been used for preparing composite hydrogels together with HEC and AA (Wang et al. 2010a, 2011a,g). The introduction of 5% APT into HEC-*g*-PAA polymeric network could improve both water absorbency and water absorption rate (Wang et al. 2010a). AA could graft onto HEC chains and the –OH groups of VMT participate in polymerization reaction. Modification of VMT by proper acidification (acidified vermiculite [AVMT]) or organification (OVMT) can improve both water absorbency and initial water absorption rate. HEC-*g*-PAA/OVMT exhibited the highest swelling capability and initial swelling rate in contrast to HEC-*g*-PAA/VMT and HEC-*g*-PAA/AVMT. Introducing 10% MS greatly enhanced the swelling capacity from 162 to 810 g/g (Wang et al. 2011e). Methylcellulose (MC) is a hydrophilic methyl ether of cellulose and has been used in pharmaceutical and food industries. Wang et al. prepared the MC-*g*-PAA/APT composite hydrogels via free radical polymerization (Wang et al. 2012b). The composite has the highest swelling ability with a weight ratio of AA to MC of 5:1 and 20% APT. Ni et al. reported an environmentally friendly slow-release nitrogen fertilizer based on APT, ethyl cellulose film, and CMC/HEC hydrogel (Ni et al. 2011). The product can reduce nutrient loss, improve use efficiency of water, and prolong irrigation cycles in drought-prone environments.

4.2.4 Sodium Alginate-Based Composite Hydrogels

Alginate, a linear polysaccharide extracted from brown seaweed, is composed of variable proportions of β-D-mannuronic acid (M block) and α-L-guluronic acid (G block) linked by 1–4 glycosidic bonds. SA is a polyelectrolyte with negative charges on its backbone and has a wide range of applications. Low flammability, foamlike materials based on ammonium alginate and MMT were fabricated through a freeze-drying process (Chen et al. 2012). These materials exhibit mechanical properties similar to those of rigid PU foams or balsa. The compressive modulus and density increase with increasing solid content, with an associated change from a layered to network microstructure structure.

Zhang et al. reported in situ generation of SA/HA nanocomposite beads as drug-controlled release matrices (Figure 4.8, Zhang et al. 2010a). The SA/HA nanocomposite beads were prepared by simultaneously carrying out the solgel transition of SA and in situ generation of HA microparticles. This is a new and simple way to decrease the release rate of drugs and overcoming the frequently observed burst release problem of drugs from hydrogel matrices. The HA microparticles were successfully generated in the beads and had a clear influence on the micromorphology. The interfacial interaction between SA and HA was greatly improved owing to the

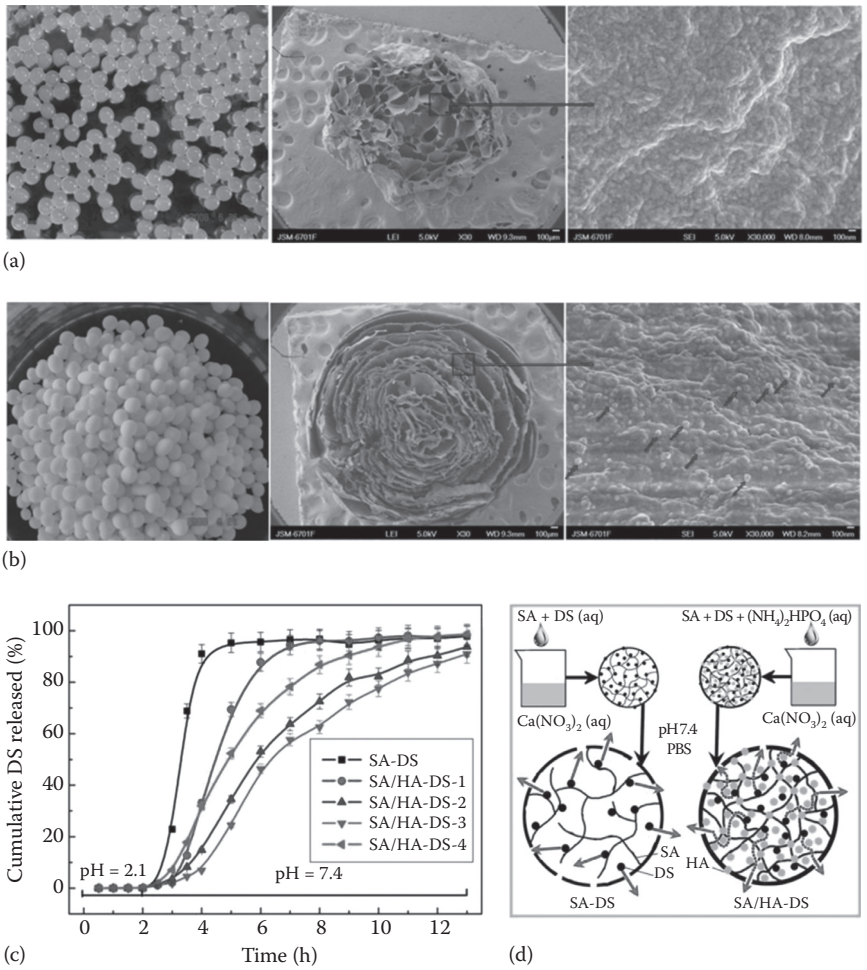

FIGURE 4.8 Digital photographs and SEM images of (a) SA and (b) SA/HA nanocomposite beads. (c) Effect of HA content on in vitro cumulative release profiles of DS from the nanocomposite beads in pH 2.1 and pH 7.4 PBS. (d) Schematic illustration of the role of HA in the nanocomposite beads. (Reprinted from *Acta Biomater.*, 6, Zhang, J.P., Wang, Q., and Wang, A.Q., In situ generation of sodium alginate/hydroxyapatite nanocomposite beads as drug controlled release matrices, 445–454, Copyright 2010, with permission from Elsevier.)

in situ generation of HA. The uniformly dispersed HA microparticles acted as inorganic cross-linkers in the nanocomposite beads and could restrict the movability of the SA polymer chains and then slow down their swelling and dissolution rates, which is also the main reason for the improved drug loading and controlled release behavior. The growth conditions of HA influence the entrapment efficiency and release rate of DS.

Clays including MMT, APT, and hydrotalcite are the most frequently used inorganic materials for the reinforcement of polymeric materials (Ray and Okamoto 2003).

Most of these clays have exchangeable cations between the anionic silicate sheets except for hydrotalcite with exchangeable anions between layers. This unique property has made it receive considerable attention recently and has been used as catalysts and organic–inorganic nanocomposites. However, the hydrotalcite-like materials, layered double hydroxides (LDHs), were frequently used instead of hydrotalcite because LDHs have the advantages of easy to be prepared and tailored, biocompatibility, low cytotoxicity, and low cost.

LDHs were also used to hybrid with SA to prepare composite hydrogels. The pH-sensitive SA/LDH hybrid beads were prepared via surface cross-linking (Zhang et al. 2010b). The positively charged LDHs are adsorbed on the negatively charged SA chains through electrostatic interaction and act as inorganic cross-linkers. Hua et al. also prepared the SA/LDH composite hydrogels by reconstruction of calcined hydrotalcite (Hua et al. 2012). Yang et al. reported a pH-sensitive nanocomposite hydrogel based on SA and APT (Yang et al. 2012). The water absorbency is as high as 694 g/g, which increased by 35% in contrast to the APT-free sample. Shi et al. prepared an SA-based composite hydrogel, SA-*g*-P(AA-*co*-St)/APT, by grafted copolymerization of AA and St onto the SA backbones in the presence of APT (Shi et al. 2012). They also reported an SA-*g*-P(AA-*co*-St)/APT superporous composite hydrogel by the grafting copolymerization and micelle templating formed by the self-assembled anionic surfactant sodium *n*-dodecyl sulfonate (SDS) (Shi et al. 2013). The SDS concentration strongly affected the morphologies and pore structure. Compared with SA-*g*-PAA hydrogel, the simultaneous introduction of a tiny amount of St and APT not only enhanced the swelling ratio but also increased the initial swelling rate. Wang et al. prepared the SA-*g*-poly(AA-*co*-sodium *p*-styrenesulfonate)/APT, SA-*g*-P(AA-*co*-NaSS)/APT, composite hydrogels (Wang et al. 2013b). The introduction of NaSS and APT could also improve the surface morphology, swelling capacity, and swelling rate. APT prefers to exist as aggregates or crystal bundles owing to electrostatic and van der Waals interactions. Thus, the unique nanometer characteristics of APT cannot be fully developed and its application was limited (Xu et al. 2011). Wang et al. disaggregated the crystal bundles of APT by the assistance of ethanol during high-pressure homogenization. The better dispersion of APT in SA-*g*-P(AA-*co*-St) improved the gel strength and swelling properties of the nanocomposite hydrogels (Figure 4.9) (Wang et al. 2013a).

MS is a special igneous rock composed of silicic acid, alumina oxide, and other elements. MS has excellent multicomponent characteristic, biological activity, and safety and has been widely applied in food science, medicine, environmental sanitation and mineral water, etc. (Juan et al. 2008). Gao et al. prepared a pH-sensitive composite hydrogel based on SA and MS (SA-*g*-PAA/MS) (Gao et al. 2011). The surface morphology and thermal stability and swelling capacity and rate of the hydrogel were clearly improved by introducing MS.

Li et al. prepared pH- and temperature-responsive semi-IPN magnetic nanocomposite hydrogels by using SA, PNIPAm, and Fe_3O_4 nanoparticles with Laponite XLG as a cross-linker (Li et al. 2012b). The hydrogels exhibited a VPTT at 32°C with no significant deviation from the conventional chemically cross-linked PNIPAm hydrogels. The swelling ratio was much higher than that of PNIPAm hydrogel. Moreover, the swelling ratio of nanocomposite hydrogels gradually decreased with

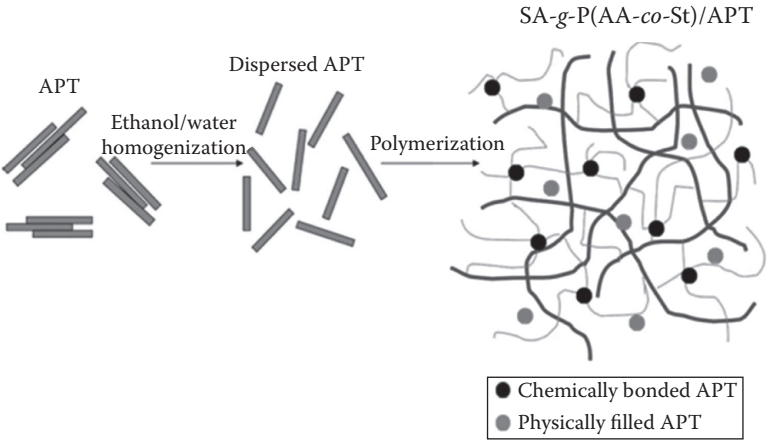

FIGURE 4.9 Schematic illustration of the formation of SA-*g*-P(AA-*co*-St)/APT nanocomposite hydrogels. (From Wang, Y.Z. et al., *Polym. Bull.*, 70, 1181, 2013b. With permission.)

increasing the content of clay and increased with increasing the content of SA. The nanocomposite hydrogels had a much better mechanical property than the PNIPAm hydrogels. The incorporation of clay did not affect the saturation magnetization of the hydrogels. A nanocomposite hydrogel with semi-interpenetrating polymer network was synthesized by in situ polymerization of NIPAm in an aqueous Laponite suspension containing SA (Wang et al. 2011d). This nanocomposite hydrogel reserved thermoresponsibility and high mechanical performance of PNIPAm–Laponite.

4.2.5 Guar Gum-Based Composite Hydrogels

Guar gum (GG), a representative natural vegetable gum, is a branched polymer with β-D-mannopyranosyl units linked (1–4) with single-membered α-D-galactopyranosyl units occurring as side branches (Wang and Wang 2009b). Recently, various inorganic materials including carbon nanotubes, silica, and clays were used to hybrid with GG for preparing functional materials (Li et al. 2012a, Singh et al. 2009). Zhang et al. prepared the MMT/carrageen/GG gel beads (Zhang et al. 2007c). The thermal stability was better than those of carrageen and GG because of the addition of MMT. MMT also reduced their solidification temperature and swelling ratio.

Wang et al. prepared a series of composite hydrogels by introducing GG and various additives (Wang et al. 2008b, Wang and Wang 2009a,b,c,d,e,f, Wang et al. 2009b, 2011g). APT, SH, MMT, VMT, REC, and MS have been incorporated into the system. The weight ratio of AA to GG and the content of additives have great influences on the swelling ability of the composite hydrogels. Wang et al. also studied the effects of modification of VMT, including organo-VMT and cation-modified VMT, on properties of the composite hydrogels (Wang et al. 2009b, 2011g). HDTMABr intercalated into the gallery layers of VMT. The intercalated VMT has been exfoliated during polymerization and uniformly dispersed in the GG-*g*-PAA matrix. HDTMA–VMT improved the swelling properties more remarkably than VMT. In addition, organo-VMT improved

the gel strength compared to VMT, and the maximum storage modulus of the nanocomposite reached 658 Pa. The cation exchange of VMT changed the interlayer gap of VMT and M^{n+} VMT was exfoliated to form a nanocomposite.

Exfoliated GG-*g*-PAA/REC composite hydrogels were obtained for acid-treated REC (H^+-REC), whereas an intercalated structure was formed for HDTMABr-modified REC (HDTMA-REC) (Wang and Wang 2009e). Modifying REC by acidification and organification can improve the water absorbency. HDTMA-REC can improve the swelling capability and swelling rate to a greater degree than H^+-REC. In the GG-*g*-PAA system, Wang and Shi et al. further introduced St to copolymerize with AA and hybrid with various additives, such as APT, MVT, VMT, and SP (Shi et al. 2011b,c,d,e, Wang et al. 2010e, Shi and Wang 2011). AA and St could graft onto the GG chain. Swelling rate and capability were enhanced by incorporating a proper amount of St and MVT (Wang et al. 2010e). Similar effects of St and APT were observed in the GG-*g*-P(AA-*co*-St)/APT system (Shi et al. 2011b,d). By using surfactant as the template, a porous fast-swelling GG-*g*-P(AA-*co*-St)/APT composite hydrogel was prepared (Shi et al. 2011b). Proper amount of SDS and nonionic surfactant *p*-octyl poly(ethylene glycol)phenyl ether can simultaneously enhance the swelling capacity and swelling rate. Yang et al. developed the GG-*g*-PAA/APT/SA pH-sensitive composite hydrogel beads for controlled drug delivery via ionic gelation (Yang et al. 2013).

4.2.6 Other Polysaccharide-Based Composite Hydrogels

Psyllium (PSY) is the common name used for several members of the plant genus Plantago. Psyllium is a gel-forming mucilage composed of a highly branched arabinoxylan. The backbone consists of xylose units, while arabinose and xylose form the side chains. The hydrogels derived from PSY have also been developed as colon-specific drug delivery agent. Singh et al. developed PSY-based hydrogels through graft copolymerization of PSY, PVA, and AA (Singh and Sharma 2010). The use of a very small amount of AA has developed the low-energy, cost-effective, biodegradable, and biocompatible material for potential biomedical applications. An et al. prepared the PSY-*g*-PAA hydrogels by graft copolymerization (An et al. 2010). On the basis of the PSY-*g*-PAA hydrogels, they also reported a series of PSY-based composite hydrogels by incorporating various clays such as APT, biotite, and MMT (An et al. 2011a,b, 2012). AA grafted onto PSY and the –OH groups of clays participated in graft polymerization. The nanocomposite containing 10% APT gives the highest water absorbency (An et al. 2012).

Kappa-carrageenan (κC), a sulfated polysaccharide, belongs to the large family of carrageenans, which are extracted from red seaweeds (An et al. 2010). Due to their excellent physical properties and biological activities, κC is extensively utilized in the food, cosmetics, textile, and pharmaceutical industries. Nanocomposite hydrogels were synthesized by copolymerization of AM and AA in the presence of carrageenan and MMT (Mahdavinia et al. 2010). The optimum water absorbency was obtained at 10% clay, 10% carrageenan, and 1:1 of monomers. They also prepared the carrageenan-*g*-PAM/Laponite RD composite hydrogels (Reza et al. 2012a).

Collagen is the most abundant protein in mammals and is composed of glycine–proline–(hydroxy)proline repeats. Collagen is frequently used for preparing hydrogels

because of its unique properties and biocompatibility. Collagen is also used to prepare nanocomposites with clays. The polypeptide/MMT nanocomposites were prepared using fish-based collagen peptide (Teramoto et al. 2007). Marandi reported the collagen-*g*-P(AA-*co*-AM)/MMT nanocomposite hydrogels (Marandi et al. 2011). MMT can improve water retention of the hydrogels under heating.

4.3 APPLICATIONS IN REMOVAL OF POLLUTANTS

Nowadays, pollution becomes a serious problem accompanying the rapid development of economy. Water pollution causes approximately 14,000 deaths per day, mostly due to the contamination of drinking water by untreated sewage in developing countries including China, India, and Zambia. Pollution in China is one aspect of the broader topic of environmental issues in China. The specific contaminants leading to water pollution include a wide spectrum of chemicals, pathogens, and physical or sensory changes. The chemical contaminants may include organic (e.g., detergents, insecticides, and dyes) and inorganic (e.g., heavy metals and ammonia) substances.

Effective pollution control is necessary to minimize the adverse effects of water pollution. Several methods including adsorption, coagulation, and precipitation have been developed to remove pollutants from wastewaters (Demirbas 2008). The adsorption method is the most frequently used because of its flexibility in design and operation as well as easy regeneration of the adsorbent. It is gradually recognized that using low-cost and environmentally friendly adsorbents to remove pollutants is an effective and economical method of water decontamination. Many materials have been used as adsorbents including CTS, clays, zeolite, and others. However, low adsorption capacity and rate are the frequently met problems for these low-cost adsorbents, which seriously restrict their applications. Approximately 3 h are needed to reach adsorption equilibrium using acid-activated APT for the removal of Cu(II) from aqueous solution (Chen et al. 2007).

Recently, the application of hydrogels as adsorbents for the removal of heavy metal ions, ammonium nitrogen, and dyes has been paid much attention (Wang et al. 2009c, Zheng and Wang 2009). Materials including CTS (Gao et al. 2013), hemicelluloses (Peng et al. 2012), polydopamine (Gao et al. 2013), and poly(dimeth yldiallylammoniumchloride)/PAM (Zheng and Wang 2010a) have been used to prepare hydrogels for the removal of pollutants in water. The flexible polymer chains and functional groups of a hydrogel make it swell partly once immersed in aqueous solution. This is convenient for the penetration of pollutants with water into the 3D network of hydrogels and bind with the functional groups. On the basis of our previous work about preparation of polysaccharide-based composite hydrogels, we studied the application of these hydrogels for the removal of pollutant from aqueous solution.

4.3.1 Removal of Heavy Metals

The main threats to human health from heavy metals are associated with exposure to lead, cadmium, mercury, and arsenic. Although several adverse health effects of heavy metals have been well known, exposure to heavy metals continues and is even increasing in some parts of the world. Meanwhile, the problem of coping

with the presence of heavy metals has become a top priority in water treatment. Various materials such as mineral apatite, mesoporous silicas, and CTS have been used for the removal of heavy metals from water (Chen et al. 1997). The transformed quantum dots showed characteristic color development, with Hg^{2+} being exceptionally identifiable due to the visible bright yellow color formation. However, there are some other problems for these adsorbent besides the aforementioned low adsorption capacity and rate. For example, CTS is an excellent adsorbent for Hg(II); however, its solubility in acid restricts its practical applications.

Hydrogels are promising materials for the removal of heavy metals. Zheng et al. reported a granular hydrogel that is an excellent adsorbent for the removal of Cu(II) and Ni(II) (Zheng and Wang 2012). Liu et al. studied the adsorption of Cu(II) using cross-linked CTS hydrogels impregnated with Congo red (CR) by ion-imprint technology (Liu et al. 2012b). Wang et al. reported the adsorption of Hg(II) ions from aqueous solution using the CTS-*g*-PAA/APT composite hydrogel (Wang and Wang 2010b). The adsorption of Hg(II) on the composites is chemical adsorption. All the –COOH, $–NH_2$, and –OH groups in the composites participate in the adsorption process. The composite can also adsorb a large amount of Hg(II) even at the very low pH_0 (pH_0 2.00). The adsorption of the composites for Hg(II) were all better fitted for the pseudo-second-order model and the Langmuir model, respectively. The values of ΔG of the composites for Hg(II) are all negative, which indicates the spontaneous nature of the adsorption process. The positive ΔH confirms that the adsorption of the composites for Hg(II) are all endothermic processes. The introduction of APT into CTS-*g*-PAA not only improves the adsorption ability and rate but also reduced the cost.

The CTS-*g*-PAA/APT composite hydrogels are also quite effective adsorbents for the removal of Cu(II) (Wang et al. 2009g). The introduction of APT into CTS-*g*-PAA could generate a loose and porous surface, which improved the adsorption ability to some extent. Compared with other adsorbents listed in Table 4.1, the equilibrium adsorption capacity of the composites are quite high. The monolayer coverage of Cu(II) on the surface of the composites was in the ascendant. The high adsorption capacity and average desorption efficiency during the consecutive five-time adsorption–desorption processes of CTS-*g*-PAA/APT composites implied that the composites possess the potential of regeneration and reuse.

Wang et al. also studied the performance of the CTS-*g*-PAA/APT composite hydrogel for the removal of Cd(II) (Wang and Wang 2010c). When $Cd(CH_3COO)_2$ was used as the solute, the equilibrium adsorption capacity was evidently larger than that of the other three cadmium salts ($Cd(NO_3)_2$, $CdCl_2$, $CdSO_4$) (Table 4.2). Results from kinetic experiments showed that Cd(II) adsorption rate on the composite was quite fast and more than 90% of Cd(II) adsorption occurred within the initial 3 min, and the adsorption equilibrium may be reached within 10 min.

The adsorption capacity of the CTS-*g*-PAA/VMT composites for Cu(II) decreases with the increase of the VMT content, but the adsorption capacity of sample with 30% VMT is still as high as 220 mg/g (Wang et al. 2010f). Wang et al. also compared the abilities of the CTS-*g*-PAA/VMT composite hydrogels to remove Pb(II) and Cd(II) ions (Wang and Wang 2012). The adsorption is fast. Ninety percent of the total adsorption was reached in 3 min for both Pb(II) and Cd(II) at 303 K, and the equilibrium was reached in 15 min. The maximum Pb(II) adsorption capacity

TABLE 4.1
Adsorption Capacity of the Adsorbents for Cu(II)

Adsorbents	Adsorption Capacity (mg/g)	Adsorbents	Adsorption Capacity (mg/g)
CTS	17.79	CTS-*g*-PAA/10% APT	243.76
N,*O*-carboxymethyl CTS	162.5	CTS-*g*-PAA/20% APT	226.95
Alumina/CTS membranes	200	CTS-*g*-PAA/50% APT	170.65
Nylon membrane	10.80	PAM/APT	104.22–115.03
Clinoptilolite	25.42	St-*g*-PAA	177.94
AC	33.12	St-*g*-PAA/5% SH	179.85
Modified pine bark	44.49	CTS-*g*-PAA/30% VMT	220
Thiourea-modified CTS	66.09	MC-*g*-PAA/5% APT	253.55
Cu(II)-imprinted composite	71.18	MC-*g*-PAA/10% APT	242.06
Acid-activated APT	32.24	MC-*g*-PAA/20% APT	231.55
CTS-*g*-PAA	262.25	MC-*g*-PAA/30% PT	166.45

Sources: Data from Zheng, Y.A. and Wang, A.Q., *J. Hazard. Mater.*, 171, 671, 2009; Zheng Y.A. et al., *Desalination*, 263, 170, 2010.

TABLE 4.2
Effect of Species of Cadmium Salts on Adsorption Capacity for Cd(II)

	Maximum Adsorption Capacity for Cd(II) (mg/g)			
Sample	**$Cd(NO_3)_2$**	**$CdCl_2$**	**$CdSO_4$**	**$Cd(CH_3COO)_2$**
CTS-*g*-PAA/30% APT	133.7	126.8	130.2	323.2

Source: Data from Wang, X.H. et al., *China Mining Mag.*, 19, 101, 2010f.

(3.08 mmol/g) of the composite is only a little more than that of Cd(II) (2.98 mmol/g). However, the desorption efficiency of Pb(II) (63.27%) is much lower than that of Cd(II) (86.26%) using 0.1 mol/L HNO_3. The adsorption of Pb(II) and Cd(II) ions by the composite seemed to involve ion exchange, chelation, electrostatic attraction, or adsorption. $–NH_2$, –COOH, and –OH groups are involved in the adsorption process. Moreover, only a few of the $–NH_2$ groups participate in the reaction with Pb(II) ions.

The CTS-*g*-PAA/SP adsorbent has a coarse, porous, and accidented surface, which is convenient for the adsorption of pollutants (Zheng et al. 2009a). The adsorption capacity of the adsorbent for Pb(II) is 638.9 mg/g, about three times of SP. After five cycles of adsorption–desorption, the adsorption capacity decreased to 489.2 mg/g, 76.6% of its original adsorption capacity. However, no adsorption can be observed after three cycles of adsorption–desorption when SP was used as the adsorbent. Shi et al. prepared the CTS-*g*-PAA/SP composite hydrogel with a specific surface area of 82.17 m^2/g, which increases the adsorption

capacity (Shi et al. 2011a). The saturated adsorption capacities of the composites for Pb(II) and Hg(II) are 286.95 and 371.89 mg/g.

The CTS-*g*-PAA/APT/SH composite hydrogels are excellent adsorbents for the removal of Pb(II) (Zhang et al. 2011, Zhang and Wang 2010). The adsorbed Pb(II) could be desorbed from the composite hydrogel efficiently using 0.05 mol/L HCl solution. In addition, the APT and SH are helpful for the recycling of the composite hydrogels, and the adsorption capacity is kept higher than 590 mg/g after five times of consecutive adsorption–desorption. The results indicate that the composite hydrogels are of high-performance, low-cost, and recyclable green adsorbents.

Szymon et al. studied the adsorption of polyvalent metal cation on the graft copolymers of potato starch with AM and AA or *N*-vinylformamide in the presence of 1%–16% MMT (Szymon et al. 2013). The adsorption of the composite was higher for Cd(II) than for Fe(III). Especially distinct differences were found for starch-based copolymers of poly(*N*-vinylformamide). Practically no influence of MMT content in the copolymers on the cation sorption was observed.

The St-*g*-PAA/SH composite hydrogels are effective for the removal of Cu(II) (Zheng et al. 2010). The composite hydrogel has higher adsorption capacity than the other adsorbents reported (Table 4.1). The addition of 5% SH into St-*g*-PAA not only improves the adsorption rate and capacity for Cu(II) but also makes the regeneration easier. The St-*g*-PAA/SH hydrogels exhibited high adsorption capacity in a wide pH range. The presence of Na^+ has no obvious effects on Cu(II) adsorption, whereas the presence of Pb(II) in the solution greatly affects the adsorption capacity. This is because the composite hydrogel adsorbs cations via complexation.

Liu et al. studied Pb(II) adsorption using the CMC-*g*-PAA/APT composite hydrogel (Liu et al. 2010a). The adsorption of Pb(II) is quite fast. Adsorption equilibrium could be reached within 60 min, and more than 90% of the equilibrium adsorption was achieved in 10 min. The adsorption process can be well described by the pseudo-second-order kinetic model, and the equilibrium adsorption isotherm was closely fitted with the Langmuir model. Complexation is the main adsorption mechanism of the composite hydrogel for Pb(II). The MC-*g*-PAA/APT composite hydrogels are ideal materials for the removal of cations (Wang et al. 2012a). Figure 4.10 shows the equilibrium absorption capacity of active carbon (AC) and the MC-*g*-PAA/APT nanocomposites with 5%, 10%, 20%, and 30% APT for Ni(II), Cu(II), and Zn(II). The adsorption capacities of the nanocomposite with 5% APT for Ni(II), Cu(II), and Zn(II) were 9.86, 7.66, and 21.86 times greater than AC, respectively. This confirmed that the chemical complexation adsorption of the nanocomposite is advantageous over the physical adsorption interaction of AC. The adsorption capacities of nanocomposite are still 6.7 (for Ni(II)), 5.01 (for Cu(II)), and 16.4 (for Zn(II)) times of AC even if the amount of APT reached 30%, which is beneficial to reduce the production cost.

Gao et al. studied the removal of heavy metal ions using the SA-*g*-PAA/MS composite hydrogels (Gao et al. 2011). Compared to AC, the adsorption capacity of the composite hydrogels for Ni(II), Cu(II), Zn(II), and Cd(II) ions increased by 10.4, 8.0, 23.0, and 14.3 fold, respectively. An et al. prepared the PSY-*g*-PAA/MMT composite hydrogels by free radical graft copolymerization, which are effective in adsorbing Cu(II) ions (An et al. 2011b).

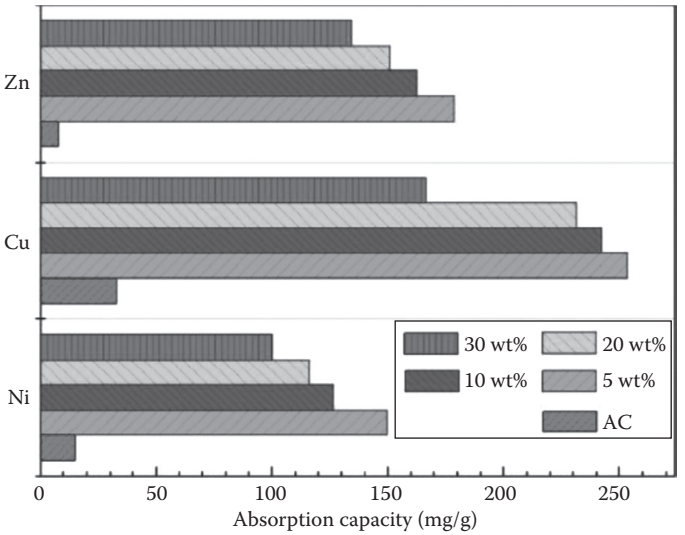

FIGURE 4.10 Absorption capacities of AC and the MC-*g*-PAA/APT nanocomposites with 5%, 10%, 20%, and 30% APT for Ni(II), Cu(II), and Zn(II) ions, respectively. (From Wang, W.B. et al., *J. Macromol. Sci. Part A*, 49, 306, 2012b. With permission.)

4.3.2 Removal of Dyes

Toxic chemical dyes are frequently used in the textile, printing, and paper industries. In China, about 1.6 billion tons of dye-containing wastewater is produced every year, but only a small proportion is recycled. Being highly colored, dyes are readily apparent in wastewater even in very low concentration. In addition, the colored wastewater can reduce the light penetration thus limiting the depuration by natural oxidation. Consequently, the presence of toxic dyes in aqueous streams poses a direct threat to the environment and humans and has gained worldwide attention. Many techniques such as ion exchange, chemical precipitation, coagulation, ozonation, and adsorption (Yan et al. 2009, Zhang et al. 2009) have been developed to remove dyes from aqueous solution. Adsorption is considered as a preferred and effective technique among these techniques as it can deal with various concentrations of dyes and it does not induce the formation of hazardous materials. The most widely employed adsorbent is AC, but the cost and difficulty in separation after adsorption hinder its large-scale application. Thus, many researchers focused on more effective adsorbents to treat dye-containing wastewater.

Despite that several low-cost adsorbents such as VMT, hazelnut shell, and rice husk ash have been investigated for decontamination purpose, the adsorption capacities of some adsorbents were restricted. So, more effective adsorbents should be attempted. Recently, because of their excellent characteristics such as high-molecular and oxygen permeability and low interfacial tension, hydrogels have attracted extensive attention for dye removal.

Wang et al. studied the removal of MB cationic dye using the CTS-*g*-PAA/APT composite hydrogels as adsorbent (Wang et al. 2011b). The adsorption rate of MB on CTS-*g*-PAA and CTS-*g*-PAA/APT with 30% APT was fast, and more than 90% of the maximum adsorption capacities were achieved within 15 min. The MB adsorption capacity is dependent on APT content, initial pH of the dye solution, and adsorption temperature. Introducing a small amount of APT could improve the adsorption ability of the CTS-*g*-PAA composite. The adsorption kinetics and isotherms were in good agreement with a pseudo-second-order equation and the Langmuir equation. The maximum adsorption capacities reached 1848 mg/g for CTS-*g*-PAA/APT. The adsorbed MB can be easily desorbed using pH 2.0 HCl solution.

Wang et al. studied the adsorption of MB using the CTS-*g*-PAA/MMT nanocomposite hydrogels (Wang et al. 2008a). The introduced MMT generates a loose and porous surface that is of benefit to the adsorption ability of the nanocomposite. The adsorption capacity of the nanocomposite for MB increased with increasing the initial pH. The weight ratio of AA to CTS has a great influence on adsorption capacities of the nanocomposites. Introducing a small amount of MMT could improve the adsorption ability of the CTS-*g*-PAA hydrogel. The maximum adsorption capacity was 1859 mg/g for CTS-*g*-PAA/MMT with 30% MMT. In desorption studies, comparatively high desorption of dyes was obtained using pH 2.0 acidic solution. So, the CTS-*g*-PAA/MMT nanocomposite hydrogel is a very effective adsorbent for the removal of MB from aqueous solution.

Liu et al. studied the adsorption of MB by the CTS-*g*-PAA/VMT composite hydrogels (Liu et al. 2010b). By introducing 10% VMT into the CTS-*g*-PAA polymeric network, the composite hydrogel showed the highest adsorption capacities for MB and could be used as a potential adsorbent for the removal of cationic dye in wastewater. They also studied the adsorption of MB by the CTS-*g*-PAA/biotite composite hydrogels (Liu et al. 2011c). The adsorption capacity calculated from the Langmuir isotherm was 2125.70 mg/g for CTS-*g*-PAA/10% biotite at 30°C. The adsorption capacity was much higher compared with other hydrogels with the same content of other clays including MMT, VMT, and APT (Table 4.3) (Liu et al. 2010b, Wang et al. 2008a, 2011b).

A granular hydrogel based on CTS and AA was prepared using Fenton reagent as the redox initiator under the ambient temperature in an air atmosphere (Figure 4.11) (Zheng et al. 2012a). The resulting networks serve as the micro- or nanoreactors for producing highly stable silver nanoparticles via in situ reduction of $AgNO_3$ with $NaBH_4$ as reducing agent and Al^{3+} as surface cross-linking agent. MB and CR with an initial concentration of 20 mg/L can be reduced completely within 30 min, and the catalytic activity is independent on initial pH and ion strength. In addition, the Ag-entrapped hydrogel shows excellent reusability for 10 successive cycles, with no appreciable decrease in the catalytic effects.

The NSC-*g*-PAM/APT composite hydrogels were quite effective adsorbents for the removal of MB (Li et al. 2011a). All the adsorption processes were better fitted by pseudo-second-order equation and the Langmuir equation. The adsorption capacity of the composite hydrogel was higher than those of CTS, APT, and many other adsorbents.

TABLE 4.3
Adsorption Capacity of Several Hydrogels for MB

Adsorbents	Adsorption Capacity (mg/g)	Adsorbents	Adsorption Capacity (mg/g)
Raw date pits	281	CTS-*g*-PAA/10% MMT	1875
H-mag	173	CTS-*g*-PAA/10% VMT	1612.32
Na-mag	331	CTS-*g*-PAA/10% APT	1870
HA-AM-PAA-B	242.4	CTS-*g*-PAA/10% BT	2125.70
Poly(*N*,*N*-dimethylacrylamide-*co*-SA)	600	CTS-*g*-PAA/10% HNTs	1034
Polymer modified biomass	869.6	CMC-*g*-PAA/5% APT	2094.80
MWS	450.0 ± 14.4	CMC-*g*-PAA/20% APT	1979.48
CMC-*g*-PAA	2153.50		

Source: Data from Liu, A.D. et al., *Biomacromolecules*, 12, 633, 2011a.

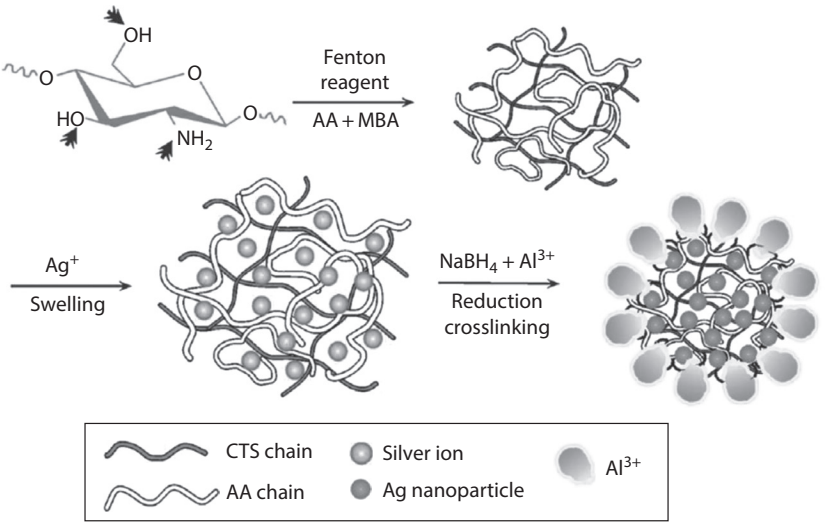

FIGURE 4.11 Schematic representation for the Ag nanoparticles formation within the hydrogel network. (Reprinted from *Chem. Eng. J.*, 179, Zheng, Y.A., Xie, Y.T., and Wang, A.Q., Rapid and wide pH-independent ammonium-nitrogen removal using a composite hydrogel with three-dimensional networks, 90–98, Copyright 2012, with permission from Elsevier.)

The CMC-*g*-PAA/APT composite hydrogel was used for the adsorption of MB (Table 4.3) (Liu et al. 2011b). The adsorption of the hydrogel for MB was quite fast, and the adsorption equilibrium could be reached within 30 min. The composite hydrogel has very high adsorption capacity for MB. The adsorption capacity is still as high as 1979.5 mg/g at 30°C even when 20% APT was introduced. The adsorbents exhibited excellent affinity for MB and can be applied to treat wastewater containing basic dyes.

4.3.3 Removal of Ammonium Nitrogen and Others

(NH_4^+-N) is an important member of the nitrogen-containing compounds that act as nutrients for aquatic plants and algae. However, if the (NH_4^+-N) level in water is too high, they can be toxic to some aquatic organisms, and if enough nutrients are present, eutrophication may occur, which is a serious problem throughout the world and poses a direct threat to public health. Therefore, the total removal or at least a significant reduction of (NH_4^+-N) in water is thus obligatory prior to disposal into streams, lakes, and seas. As the convenient and effective approach, natural or modified zeolite and molecular sieve have been used as the adsorbents to remove (NH_4^+-N) in water. However, the adsorption capacity is too low to satisfy the effective demand.

Hydrogels were also promising materials for the removal of (NH_4^+-N). Yuan and Kusuda used a poly(NIPAm-*co*-chlorophyllin) hydrogel to adsorb (NH_4^+-N). The hydrogel had an adsorption capacity of 0.18 mg/g for (NH_4^+-N) (Yuan and Kusuda 2005). Zheng et al. reported that the adsorption of CTS-*g*-PAA/APT composite hydrogel for (NH_4^+-N) is pH dependent and has faster adsorption kinetics and higher adsorption capacity than the other adsorbents (Table 4.4) (Zheng et al. 2009). At natural pH, the composite adsorbent with 20% APT can adsorb 21.0 mg NH_4^+-N per gram of adsorbent. The adsorption capacity increased with increasing APT content up to an optimum result of 20% and then decreased with further increase in APT content. The adsorption is attributed to the $–COO^-$ groups within the polymeric network. Adsorption of NH_4^+-N is mainly controlled by the electrostatic attraction between the $–COO^-$ groups and the positively charged NH_4^+-N. Owing to the reactive –OH groups, an appropriate addition of APT could enlarge the surface area and porosity of the adsorbent and contribute to its higher adsorption capacity.

Zheng et al. reported the usage of the CTS-*g*-PAA/REC composite hydrogel for the removal of NH_4^+-N from water (Zheng and Wang 2009). The adsorption equilibrium can be obtained within 3–5 min. The monolayer adsorption

TABLE 4.4
Adsorption Capacity of Various Adsorbents for NH_4^+-N

Adsorbents	Adsorption Capacity (mg/g)	Adsorbents	Adsorption Capacity (mg/g)
CTS-*g*-PAA/20% APT	21.0	Zeolite 13X	8.61
MMT	7.8	Activated sludge	0.4–0.5
Kaolin	5.5	PNIPAm	0.08
APT	8.5	Poly(NIPAm-*co*-chlorophyllin)	0.18
REC	6.4	CTS-*g*-PAA	109.2
PAC	5.7	CTS-*g*-PAA/10% REC	123.8
Natural zeolite	1.0–1.5	CTS-*g*-PAA/30% REC	61.95
Clinoptilolite	8.96	CTS-*g*-PAA/HNTs	27.7

Source: Data from Zheng, Y.A. et al., *Chem. Eng. J.*, 155, 215, 2009b.

is 109.2, 123.8, and 61.95 mg/g for CTS-*g*-PAA, CTS-*g*-PAA/10% REC, and CTS-*g*-PAA/30%REC, respectively, meaning high adsorption capacity for NH_4^+ removal. This hydrogel can be extensively used in a wide pH range from 4.0 to 9.0, and external temperature has little effects on the adsorption capacity, suggesting that the adsorbent is applicable to a large class of adsorption systems. Cations, especially multivalent cations, which coexisted with NH_4^+ in the solution, can have some negative effects on the adsorption capacity of CTS-*g*-PAA/REC. However, the adsorption capacity for NH_4^+-N is still higher than 30 mg/g even with the existence of high-concentration saline solutions (0.5 mmol/L). The adsorbent can be regenerated by desorption of NH_4^+-N. The regeneration condition is mild and the recovered adsorbent can be used again. In addition, more adsorption sites would be created during the regeneration.

The CTS-*g*-PAA/HNT composite hydrogels also can remove NH_4^+-N from synthetic wastewater (Zheng and Wang 2010c). By introducing HNTs into the polymeric networks, the composite shows comparable adsorption capacity to that of pure polymer hydrogel. The adsorption equilibrium can be achieved within 5 min with the equilibrium adsorption capacity of 27.7 mg/g. The adsorption process is pH independent within 4.0–7.0, and the adsorption capacity of the as-prepared adsorbent is not affected over the five cycles of adsorption.

Zheng et al. found that the CTS-*g*-PAA/VMT composite hydrogels are rapid and wide pH-independent NH_4^+-N adsorbents (Figure 4.12) (Zheng et al. 2012). The adsorption equilibrium can be achieved in a few minutes and the maximum, constant adsorption capacity can be observed in a wide pH range of 4.0–8.0. The adsorbent can exclusively adsorb NH_4^+-N in the mixing solution containing NH_4^+-N and PO_4^{3-} P, suggesting that the electrostatic attraction dominates the whole adsorption process.

The ion cross-linked CTS-*g*-PAA/VMT composite hydrogels were applied for the removal of phosphate ions from aqueous solution (Zheng and Wang 2010b). The trivalent ion cross-linked hydrogel exhibited a potential for the removal of phosphate ions. A lower pH is convenient for the adsorption of phosphate ions onto the adsorbent. The maximum adsorption capacity of 22.64 mg/g was comparable with that reported for other adsorbents (Table 4.5).

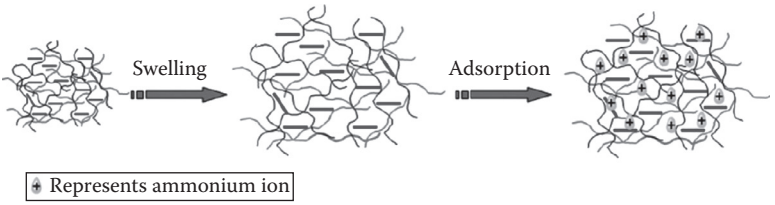

FIGURE 4.12 Model scheme for the adsorption of NH_4^+-N onto CTS-*g*-PAA/VMT. (Reprinted from *Chem. Eng. J.*, 179, Zheng, Y.A., Xie, Y.T., and Wang, A.Q., Rapid and wide pH-independent ammonium-nitrogen removal using a composite hydrogel with three-dimensional networks, 90–98, Copyright 2012, with permission from Elsevier.)

TABLE 4.5
Adsorption Capacity of Various Adsorbents for Phosphate

Adsorbents	Adsorption Capacity (mg/g)	Reference
Al-CPV	22.64	Zheng and Wang (2010a)
Za-ZFA	35.31	Wu et al. (2006)
Iron oxide tailing	8.21	Zeng et al. (2004)
Aluminum oxide	35.03	Borggaard et al. (2005)
Steel furnace slag	1.43	Sakadevan and Bavor (1998)
Natural zeolite	0.46	Drizo (1998)
DMAEMA-*g*-PP	11.4[a]	Taleb et al. (2008)
Ammonium-functionalized MCM-48	35.4[b]	Saad et al. (2007)
Mesoporous ZrO_2	29.71	Liu et al. (2008)
Iron oxide/fly ash composite	27.39	Yao et al. (2009)

Source: Zheng, Y.A. and Wang, A.Q., *Adsorpt. Sci. Technol.*, 28, 89, 2010b.

[a] Initial phosphate concentration, 100 mg/L.

[b] Initial phosphate concentration, 300 mg/L.

4.4 CONCLUDING REMARKS AND PERSPECTIVES

Polysaccharide-based composite hydrogels with novel properties develop very quickly recently. Polysaccharides including CTS, cellulose, starch, SA, and GG have been used for preparing the composite hydrogels. Various clays with different structure and properties such as APT, MMT, VMT, and Laponite were introduced into the polymeric 3D network.

Owing to the synergistic effect among polysaccharide, vinyl monomer, and clay mineral, many of the physicochemical properties such as swelling ratio and rate, thermostability, and gel strength of the composite hydrogels are superior to their counterparts. The –OH and $–NH_2$ groups of many polysaccharides take part in graft polymerization with the vinyl monomers. The –OH groups of clay minerals may also react with the monomers and interact with polysaccharides and grafted hydrophilic polymers via hydrogen bonding. Clays could form physical cross-linking points in the hydrogel network and have great influences on the surface morphology and then affect the swelling behaviors. This is related to morphology, microstructure, and physicochemical properties of the clay.

The polysaccharide-based composite hydrogels are rich in functional groups, for example, –OH, $–COO^-$, –COOH, $–NH_2$, and $–CONH_2$, and show promising application in the removal of pollutants from water. The adsorption capacities of the composite hydrogels are very high for heavy metal ions, dyes, and NH_4^+-N compared to the traditional adsorbents such as AC and clays. Swelling of the composite hydrogels is helpful for the penetration of pollutant molecules into the hydrogel network and their interaction between the functional groups. This makes the adsorption very fast and the adsorption capacity very high.

Most of the studies introduce clays directly into the polymeric network. Thus, the compatibility of polymer and clays remains to be improved. Modification of clay with proper reagents is helpful to improve their compatibility.

Before using for practical applications, some problems need to be solved for the polysaccharide-based composite hydrogels. Effort in this area is still needed in order to further optimize the composite hydrogel's performance in the future. (1) A proper swelling degree of the composite is helpful to enhance the adsorption capacity and rate. However, too high swelling ratio will result in handling difficulty after adsorption. Thus, further cross-linking points are necessary to maintain proper swelling ratio while keeping their excellent adsorption capacity. (2) Most of the reports studied the adsorption capacity with very high concentration of the pollutants, which is far from practical applications. The concentration of metal ions in industrial wastewater is not very high, for example, below 10 ppm for Ni (II). Thus, further studies should focus on the application of the composite hydrogels for the removal of pollutants at low concentration. (3) The reusability still needs to be improved, although many composite hydrogels show good adsorption capacity after five adsorption–desorption recycles. Stability for even more cycles should be investigated. In addition, the repeating adsorption–desorption will result in decrease of their gel strength and partly loss of the composite hydrogels, which should be addressed in further studies. The dissolved composite hydrogels may result in secondary pollution and must be avoided. (4) The selectivity of the composite hydrogels for pollutants is also very important for their practical applications. The coexistence of many other metal ions and compounds in various forms will make the adsorption process very complicated. Thus, composite hydrogels with excellent selectivity for pollutants are in high demand and should become a focus in further studies.

ABBREVIATIONS

AA	Acrylic acid
AC	Active carbon
AM	Acrylamide
APT	Attapulgite
CMC	Carboxymethyl cellulose
CR	Congo red
CTS	Chitosan
CV	Crystal violet
CVNH_4^+-N	Crystal violet ammonium nitrogen
DS	Diclofenac sodium
GDL	Gluconolactone
GG	Guar gum
HA	Hydroxyapatite
HDTMABr	Hexadecyltrimethylammonium bromide
HEC	Hydroxyethyl cellulose
HEMA	2-Hydroxyethyl methacrylate

HES	Hydroxyethyl starch
HESDS	Hydroxyethyl starch diclofenac sodium
HNTs	Halloysite nanotubes
κC	Kappa-carrageenan
LDHs	Layered double hydroxides
MB	Methylene blue
MBA	*N*,*N*′-methylenebisacrylamide
MC	Methylcellulose
MMT	Montmorillonite
MS	Medical stone
NH_4^+-N	Ammonium nitrogen
NIPAm	*N*-Isopropylacrylamide
OFL	Ofloxacin
PAM	Polyacrylamide
PSY	Psyllium
REC	Rectorite
SA	Sodium alginate
SDS	Sodium *n*-dodecyl sulfonate
SH	Sodium humate
SP	Sepiolite
St	Styrene
TPP	Sodium tripolyphosphate
TPS	Thermoplastic starch
VMT	Vermiculite
VPTT	Phase transition temperature

REFERENCES

An, J.K., W.B. Wang, and A.Q. Wang. 2010. Preparation and swelling properties of a pH-sensitive superabsorbent hydrogel based on psyllium gum. *Starch/Stärke* 62: 501–507.

An, J.K., W.B. Wang, and A.Q. Wang. 2011a. Preparation and swelling properties of ph responsive psyllium-graft-poly(acrylic acid)/biotite superabsorbent composites. *Polym. Mater. Sci. Eng.* 27: 31–34.

An, J.K., W.B. Wang, and A.Q. Wang. 2011b. Preparation of psyllium gum-*g*-poly(acrylic acid)/Na-montmorillonite supersorbent composites and its adsorption performance for Cu^{2+}. *J. Funct. Polym*. 24: 186–190.

An, J.K., W.B. Wang, and A.Q. Wang. 2012. Preparation and swelling behavior of a pH-responsive psyllium-*g*-poly(acrylic acid)/attapulgite superabsorbent nanocomposite. *Int. J. Polym. Mater*. 61: 906–918.

Borggaard, O.K., B. Raben-Lange, A.L. Gimsing, and B.W. Strobel. 2005. Influence of humic substances on phosphate adsorption by aluminium and iron oxides. *Geoderma* 127: 270–279.

Bradley, W.F. 1940. The structural scheme of attapulgite. *Am. Miner.* 25: 405–410.

Chen, H., W.B. Wang, and A.Q. Wang. 2010. Preparation and swelling behaviors of CMC-*g*-PAA/APT/HA superabsorbent composites. *Humic Acid* 5: 5–10.

Chen, H., Y.G. Zhao, and A.Q. Wang. 2007. Removal of Cu(II) from aqueous solution by adsorption onto acid-activated palygorskite. *J. Hazard. Mater.* 149: 346–354.

Chen, H.B., Y.T. Wang, M. Sánchez-Sotoc, and D.A. Schiraldi. 2012. Low flammability, foam-like materials based on ammonium alginate and sodium montmorillonite clay. *Polymer* 53: 5825–5831.

Chen, X.B., J.V. Wright, J.L. Conca, and L.M. Peurrung. 1997. Effects of pH on heavy metal sorption on mineral apatite. *Environ. Sci. Technol.* 31: 624–631.

Chivrac, F., E. Pollet, M. Schmutz, and L. Avérous. 2008. New approach to elaborate exfoliated starch-based nanobiocomposites. *Biomacromolecules* 9: 896–900.

Dawson, J.I., J.M. Kanczler, X.B.B. Yang, G.S. Attard, and R.O.C. Oreffo. 2011. Skeletal regeneration: Application of nanotopography and biomaterials for skeletal stem cell based bone repair. *Adv. Mater.* 23: 3304–3308.

Deen, I., X. Pang, and I. Zhitomirsky. 2012. Electrophoretic deposition of composite chitosan–halloysite nanotube–hydroxyapatite films. *Colloids Surf. A* 410: 38–44.

Demirbas, A. 2008. Heavy metal adsorption onto agro-based waste materials: A review. *J. Hazard. Mater*. 157: 220–229.

Drizo, A., C.A. Frost, K.A. Smith, and J. Grace. 1998. Phosphate and ammonium removal by constructed wetlands with horizontal subsurface flow, using shale as a substrate. *Water Res*. 35: 95–102.

Gao, H.C., Y.M. Sun, J.J. Zhou, R. Xu, and H.W. Duan. 2013. Mussel-inspired synthesis of polydopamine-functionalized graphene hydrogel as reusable adsorbents for water purification. *ACS Appl. Mater. Interfaces* 5: 425–432.

Gao, T.P., W.B. Wang, and A.Q. Wang. 2011. A pH-sensitive composite hydrogel based on sodium alginate and medical stone: Synthesis, swelling and heavy metal ions adsorption properties. *Macromol. Res.* 19: 739–748.

Hayes, M.H.B., P. MacCarthy, R.L. Malcolm, and R.S. Swift (eds.). *Humic Substances II: In Search of Structure*. Chichester, U.K.: Wiley; 1989.

Hua, S.B. and A.Q. Wang. 2008. Preparation and properties of superabsorbent containing starch and sodium humate. *Polym. Adv. Technol.* 19: 1009–1014.

Hua, S.B., H.X. Yang, and A.Q. Wang. 2008. A pH-sensitive nanocomposite microsphere based on chitosan and montmorillonite with in vitro reduction of the burst release effect. *Drug Dev. Ind. Pharm*. 36: 1106–1114.

Hua, S.B., H.X. Yang, W.B. Wang, and A.Q. Wang. 2010. Controlled release of ofloxacin from chitosan–montmorillonite hydrogel. *Appl. Clay Sci*. 50: 112–117.

Hua, S.B., H.X. Yang, J.P. Zhang, and A.Q. Wang. 2012. Preparation and swelling properties of pH-sensitive sodium alginate/layered double hydroxides hybrid beads for controlled release of diclofenac sodium. *Drug Dev. Ind. Pharm.* 38: 728–734.

Huang, D.J., B. Mu, and A.Q. Wang. 2012a. Preparation and properties of chitosan/poly (vinyl alcohol) nanocomposite films reinforced with rod-like sepiolite. *Mater. Lett.* 86: 69–72.

Huang, W., H.J.L. Xu, Y. Xue, R. Huang, H.B. Deng, and S.Y. Pan. 2012b. Layer-by-layer immobilization of lysozome-chitosan-organic rectorite composites on electrospun nanofibrous mats for pork preservation. *Food Res. Int.* 48: 784–791.

Huang, Y.S., S.H. Yu, Y.R. Sheu, and K.S. Huang. 2010. Preparation and thermal and anti-UV properties of chitosan/mica copolymer. *J. Nanomater.* 2010: 65–71.

Juan, L., P.Y. Zhang, Y. Gao, X.G. Song, and J.H. Dong. 2008. Overview of Maifanshi: Its physi-chemical properties and nutritious function in drinking water. *Environ. Sci. Technol.* 31: 63–67.

Klien, C., B. Dutrow, and J.D. Dana. *Manual of Mineral Science*, 23rd edn. Hoboken, NJ: John Wiley & Sons, Inc.,; 2008.

Li, A., R.F. Liu, and A.Q. Wang. 2005. Preparation of starch–graft–poly (acrylamide)/attapulgite superabsorbent composite. *J. Appl. Polym. Sci*. 98: 1351.

Li, A., A.Q. Wang, and J.M. Chen. 2004. Studies on poly(acrylic acid)/attapulgite superabsorbent composite. I. Synthesis and characterization. *J. Appl. Polym. Sci.* 92: 1596–1603.

Li, A., J.P. Zhang, and A.Q. Wang. 2007a. Utilization of starch and clay for the preparation of superabsorbent composite. *Bioresour. Technol.* 98: 327–332.

Li, J.F., Y.M. Li, and H.P. Dong. 2008. Controlled release of herbicide acetochlor from clay/carboxylmethilcellulose gel formulations. *J. Agric. Food Chem*. 56: 1336–1342.

Li, P., J.P. Zhang, and A.Q. Wang. 2007b. A novel succinyl-chitosan-*g*-polyacrylamide/attapulgite composite hydrogel prepared through inverse suspension polymerization. *Macromol. Mater. Eng.* 292: 962–969.

Li, Q., Y.H. Zhao, L. Wang, and A.Q. Wang. 2011a. Adsorption characteristics of methylene blue onto the *N*-succinyl-chitosan-*g*-polyacrylamide/attapulgite composite. *Korean J. Chem. Eng.* 28: 1658–1664.

Li, X.X., X.Y. Li, B.L. Ke, X.W. Shi, and Y.M. Du. 2011b. Cooperative performance of chitin whisker and rectorite fillers on chitosan films. *Carbohydr. Polym.* 85: 747–752.

Li, Y., P.R. Chang, P.W. Zheng, and X.F. Ma. 2012a. Characterization of magnetic guar gum-grafted carbon nanotubes and the adsorption of the dyes. *Carbohydr. Polym*. 87: 1919–1924.

Li, Z.Q., J.F. Shen, H.W. Ma, X. Lu, M. Shi, N. Li, and M.X. Ye. 2012b. Preparation and characterization of sodium alginate/poly(*N*-isopropylacrylamide)/clay semi-IPN magnetic hydrogels. *Polym. Bull.* 68: 1153–1169.

Lin, J.M., J.H. Wu, Z.F. Yang, and M.L. Pu. 2001. Synthesis and properties of poly(acrylic acid)/mica superabsorbent nanocomposite. *Macromol. Rapid Commun*. 22: 422–424.

Liu, A.D., A. Walther, O. Ikkala, L. Belova, and A. Lars Berglund. 2011a. Clay nanopaper with tough cellulose nanofiber matrix for fire retardancy and gas barrier functions. *Biomacromolecules* 12: 633–641.

Liu, B., X.Y. Wang, X.Y. Li, X.J. Zeng, R.C. Sun, and J.F. Kennedy. 2012a. Rapid exfoliation of rectorite in quaternized carboxymethyl chitosan. *Carbohydr. Polym.* 90: 1826–1830.

Liu, B., X.Y. Wang, C.S. Pang, J.W. Luo, Y.Q. Luo, and R.C. Sun. 2013a. Preparation and antimicrobial property of chitosan oligosaccharide derivative/rectorite nanocomposite. *Carbohydr. Polym.* 92: 1078–1085.

Liu, H., X. Sun, C. Yin, and C. Hu. 2008. Removal of phosphate by mesoporous ZrO_2. *J. Hazard. Mater.* 151: 616–622.

Liu, J.H. and A.Q. Wang. 2008a. Synthesis & water retention of chitosan-*g*-poly(acrylic acid)/rectorite superabsorbent composites. *Non-Metallic Mines* 31: 37–40.

Liu, J.H. and A.Q. Wang. 2008b. Synthesis, characterization and swelling behaviors of chitosan-*g*-poly(acrylic acid)/organo-rectorite nanocomposite superabsorbents. *J. Appl. Polym. Sci.* 110: 678–686.

Liu, J.H., Q. Wang, and A.Q. Wang. 2007. Synthesis and characterization of chitosan-*g*-poly(acrylic acid)/sodium humate superabsorbent. *Carbohydr. Polym.* 70: 166–173.

Liu, Y., H. Chen, J.P. Zhang, and A.Q. Wang. 2013b. Effect of number of grindings of attapulgite on enhanced swelling properties of the superabsorbent nanocomposites. *J. Compos. Mater.* 47: 969–978.

Liu, Y., Y.R. Kang, D.J. Huang, and A.Q. Wang. 2012b. Cu^{2+} removal from aqueous solution by modified chitosan hydrogels. *J. Chem. Technol. Biotechnol.* 87: 1010–1016.

Liu, Y., W.B. Wang, Y.L. Jin, and A.Q. Wang. 2011b. Adsorption behavior of methylene blue from aqueous solution on the hydrogel composites based on carboxymethyl cellulose and attapulgite. *Sep. Sci. Technol.* 46: 858–868.

Liu, Y., W.B. Wang, and A.Q. Wang. 2010a. Adsorption of lead ions from aqueous solution by using carboxymethyl cellulose-*g*-poly (acrylic acid)/attapulgite hydrogel composites. *Desalination* 259: 258–264.

Liu, Y., Y.A. Zheng, and A.Q. Wang. 2010b. Enhanced adsorption of methylene blue from aqueous solution by chitosan-*g*-poly (acrylic acid)/vermiculite hydrogel composites. *J. Environ. Sci*. 22: 486–493.

Liu, Y., Y.A. Zheng, and A.Q. Wang. 2011c. Effect of biotite of hydrogels on enhanced removal of cationic dye from aqueous solution. *Ionics* 17: 535–543.

Liu, Y., Y.A. Zheng, and A.Q. Wang. 2011d. Response surface methodology for optimizing adsorption process parameters for methylene blue removal by hydrogel composite. *Adsorpt. Sci. Technol.* 28: 913–922.

Luo, W., W.A. Zhang, and P. Chen. 2005. *Co*-(acrylic acid)/montmorillonite nanosuperabsorbent via gamma-ray irradiation technique. *J. Appl. Polym. Sci*. 96: 1341–1346.

Lutolf, M.P. and J.A. Hubbell. 2005. Synthetic biomaterials as instructive extracellular microenvironments for morphogenesis in tissue engineering. *Nat. Biotechnol*. 23: 47–55.

Ma, J.H., Y.J. Xu, Q.S. Zhang, L.S. Zha, and B. Liang. 2007. Preparation and characterization of pH- and temperature-responsive semi-IPN hydrogels of carboxymethyl chitosan with poly(*N*-isopropylacrylamide) crosslinked by clay. *Colloid Polym. Sci.* 285: 479–484.

Ma, J.H., L. Zhang, B. Fan, Y.J. Xu, and B.R. Liang. 2008. A novel sodium carboxymethylcellulose/poly(*N*-isopropylacrylamide)/clay semi-IPN nanocomposite hydrogel with improved response rate and mechanical properties. *J. Polym. Sci. Part B: Polym. Phys.* 46: 1546–1555.

Marandi, G.B., G.R. Mahdavinia, and S. Ghafary. 2011. Collagen-*g*-poly(sodium acrylate-*co*-acrylamide)/sodium montmorillonite superabsorbent nanocomposites: Synthesis and swelling behavior. *J. Polym. Res.* 18: 1487–1499.

Margarita, D., L.B. Mar, A. Pilar, J.A. Antonio, B. Julio, and R.H. Eduardo. 2006. Microfibrous chitosan-sepiolite nanocomposites. *Chem. Mater.* 18: 1602–1610.

Margarita, D., C. Montserrat, and R.H. Eduardo. 2003. Biopolymer-clay nanocomposites based on chitosan intercalated in montmorillonite. *Chem. Mater*. 15: 3774–3780.

Neaman, A. and A. Singer. 2004. Possible use of the Sacalum (Yucatan) palygorskite as drilling muds. *Appl. Clay Sci.* 25: 121–124.

Ni, B.L., M.Z. Liu, S.Y. Lü, L.H. Xie, and Y.F. Wang. 2011. Environmentally friendly slow-release nitrogen fertilizer. *J. Agric. Food Chem.* 59: 10169–10175.

Peng, X.W., L.X. Zhong, J.L. Ren, and R.C. Sun. 2012. Synthesis and characterization of amphoteric xylan-type hemicelluloses by microwave irradiation. *J. Agric. Food Chem.* 60: 3909–3916.

Perotti, G.F., H.S. Barud, Y. Messaddeq, S.J.L. Ribeiro, and R.L. Constantino Vera. 2011. Bacterial cellulose–laponite clay nanocomposites. *Polymer* 52: 157–163.

Ray, S.S. and M. Okamoto. 2003. Polymer/layered silicate nanocomposites: Structure formation, interactions and deformation mechanisms. *Prog. Polym. Sci*. 28: 1539–1641.

Reza, M.G., M. Abdolhossein, B. Ali, and M. Bakhshali. 2012a. Novel carrageenan-based hydrogel nanocomposites containing laponite RD and their application to remove cationic dye. *Iran. Polym. J*. 21: 609–619.

Saad, R., K. Belkacemi, and S. Hamoudi. 2007. Adsorption of phosphate and nitrate anions on ammonium-functionalised MCM-48: Effects of experimental conditions. *J. Colloid Interface Sci.* 311: 375–381.

Sakadevan, K. and H. Bavor. 1998. Phosphate adsorption characteristics of soils, slags and zeolite to be used as substrates in constructed wetland systems. *Water Res.* 32: 393–398.

Shang, J., Z.Z. Shao, and X. Chen. 2008. Electrical behavior of a natural polyelectrolyte hydrogel: Chitosan/carboxymethylcellulose hydrogel. *Biomacromolecules* 9: 1208–1213.

Shchukin, D.G., S.V. Lamaka, K.A. Yasakau, M.L. Zheludkevich, M.G.S. Ferreira, and H. Möhwald. 2008. Active anticorrosion coatings with halloysite nanocontainers. *J. Phys. Chem. C* 112: 958–964.

Shi, J.W. 2011. Synthesis and adsorption performance of CTS-*g*-poly(acrylic acid)/sepiolite composites. Master's thesis, Chengdu University of Technology, Chengdu, China, p. 6.

Shi, X.N. and A.Q. Wang. 2011. Synthesis and swelling properties of guar gum-*g*-poly(sodium acrylate-*co*-styrene)/sepiolite superabsorbent composite. *J. Chem. Ind. Eng*. 62: 864–869.

Shi, X.N, W.B. Wang, Y.R. Kang, and A.Q. Wang. 2012. Enhanced swelling properties of a novel sodium alginate-based superabsorbent composites: NaAlg-*g*-poly(NaA-*co*-St)/APT. *J. Appl. Polym. Sci.* 125: 1822–1832.

Shi, X.N., W.B. Wang, and A.Q. Wang. 2011a. Effect of surfactant on porosity and swelling behaviors of guar gum-*g*-poly(sodium acrylate-*co*-styrene)/attapulgite superabsorbent hydrogels. *Colloids Surf. B* 88: 279–286.

Shi, X.N., W.B. Wang, and A.Q. Wang. 2011b. Swelling behavior of guar gum-*g*-poly(sodium acrylate-*co*-styrene)/attapulgite superabsorbent composites. *J. Macromol. Sci. B* 50: 1847–1863.

Shi, X.N., W.B. Wang, and A.Q. Wang. 2011c. Synthesis and enhanced swelling properties of a guar gum-based superabsorbent composite by the simultaneous introduction of styrene and attapulgite. *J. Polym. Res.* 18: 1705–1713.

Shi, X.N, W.B. Wang, and A.Q. Wang. 2011d. Synthesis, characterization and swelling behaviors of guar gum-*g*-poly(sodium acrylate-*co*-styrene)/vermiculite superabsorbent composites. *J. Compos. Mater.* 45: 2189–2198.

Shi, X.N., W.B. Wang, and A.Q. Wang. 2013. pH-responsive sodium alginate-based superporous hydrogel generated by an anionic surfactant micelle templating. *Carbohydr. Polym.* 94: 449–455.

Singh, B. and V. Sharma. 2010. Design of psyllium-PVA-acrylic acid based novel hydrogels for use in antibiotic drug delivery. *Int. J. Pharm.* 389: 94–106.

Singh, V., S. Pandey, S.K. Singh, and R. Sanghi. 2009. Removal of cadmium from aqueous solutions by adsorption using poly(acrylamide) modified guar gum–silica nanocomposites. *Sep. Purif. Technol.* 67: 251–261.

Sun, J.Y., X. Zhao, W.R. Illeperuma, O. Chaudhuri, K.H. Oh, D.J. Mooney, J.J. Vlassak, and Z. Suo. 2012. Highly stretchable and tough hydrogels. *Nature* 489: 133–136.

Taleb, M.F.A., G.A. Mahmoud, S.M. Elsigeny, and E.A. Hegazy. 2008. Adsorption and desorption of phosphorus and nitrate ions using quaternary (polypropylene-*g*-*N*,*N*-dimethylaminoethyl methacrylate) graft copolymer. *J. Hazard. Mater.* 159: 372–379.

Tekin, N., A. Dinçer, Ő. Demirbaş, and M. Alkan. 2006. Adsorption of cation polyacrylamide onto sepiolite. *J. Hazard. Mater*. B134: 211–219.

Teramoto, N., D. Uchiumi, A. Niikura, Y. Someya, and M. Shibata. 2007. Polypeptide/layered silicate nanocomposites using fish-based collagen peptide: Effect of crosslinking and chain extension of the collagen peptide. *J. Appl. Polym. Sci.* 106: 4024–4030.

Wang, A.Q. and W.B. Wang. 2009a. Superabsorbent materials. *Kirk-Othmer Encyclopedia of Chemical Technology*. Wiley, New York, pp. 1–34.

Wang, J.L., W.B. Wang, and A.Q. Wang. 2010a. Synthesis, characterization and swelling behaviors of hydroxyethyl cellulose-*g*-poly(acrylic acid)/attapulgite superabsorbent composite. *Polym. Eng. Sci.* 50: 1019–1027.

Wang, J.L., W.B. Wang, Y.A. Zheng, and A.Q. Wang. 2011a. Effects of modified vermiculite on the synthesis and swelling behaviors of hydroxyethyl cellulose-*g*-poly(acrylic acid)/vermiculite superabsorbent nanocomposites. *J. Polym. Res.* 18: 401–408.

Wang, L. and A.Q. Wang. 2008. Adsorption behaviors of Congo red on the N, *O*-carboxymethyl-chitosan/montmorillonite nanocomposite. *Chem. Eng. J.* 143: 43–50.

Wang, L., J.P. Zhang, and A.Q. Wang. 2008a. Removal of methylene blue from aqueous solution using chitosan-*g*-poly(acrylic acid)/montmorillonite superadsorbent nanocomposite. *Colloids Surf. A.* 322: 47–53.

Wang, L., J.P. Zhang, and A.Q. Wang. 2011b. Fast removal of methylene blue from aqueous solution by adsorption onto chitosan-*g*-poly (acrylic acid)/attapulgite composite. *Desalination* 266: 33–39.

Wang, Q., W.B. Wang, J. Wu, and A.Q. Wang. 2012a. Effect of attapulgite contents on release behaviors of a pH sensitive carboxymethyl cellulose-*g*-poly (acrylic acid)/attapulgite/sodium alginate composite hydrogel bead containing diclofenac. *J. Appl. Polym. Sci.* 124: 4424–4432.

Wang, Q., J. Wu, W.B. Wang, and A.Q. Wang. 2011c. Preparation, characterization and drug-release behaviors of crosslinked chitosan/attapulgite hybrid microspheres by a facile spray-drying technique. *J. Biol. Nanobiotechnol.* 2: 250–257.

Wang, Q., X.L. Xie, X.W. Zhang, J.P. Zhang, and A.Q. Wang. 2010b. Preparation and swelling properties of pH sensitive composite hydrogel beads based on chitosan-*g*-poly (acrylic acid)/vermiculite and sodium alginate for diclofenac controlled release. *Int. J. Biol. Macromol.* 46: 356–362.

Wang, Q., J.P. Zhang, and A.Q. Wang. 2009a. Preparation and characterization of a novel pH-sensitive chitosan-*g*-poly(acrylic acid)/attapulgite/sodium alginate composite hydrogel bead for controlled release of diclofenac sodium. *Carbohydr. Polym.* 78: 731–737.

Wang, Q., J.P. Zhang, and A.Q. Wang. 2010c. Preparation and properties of drug loaded hydrogel beads based on halloysite. *Chem. Res. Appl.* 22: 858–863.

Wang, Q.G., J.L. Mynar, M. Yoshida, E. Lee, M. Lee, K. Okuro, K. Kinbara, and T. Aida. 2010d. High-water-content mouldable hydrogels by mixing clay and a dendritic molecular binder. *Nature* 463: 339–343.

Wang, T., D. Liu, C.X. Lian, S.D. Zheng, X.X. Liu, C.Y. Wang, and Z. Tong. 2011d. Rapid cell sheet detachment from alginate semi-interpenetrating nanocomposite hydrogels of PNIPAm and hectorite clay. *React. Funct. Polym.* 71: 447–454.

Wang, W.B., Y.R. Kang, and A.Q. Wang. 2010e. Synthesis, characterization and swelling properties of the guar gum-*g*-poly(sodium acrylate-*co*-styrene)/muscovite superabsorbent composites. *Sci. Technol. Adv. Mater.* 11: 025006.

Wang, W.B. and A.Q. Wang. 2009b. Effects of crosslinking degree on the properties of guar gum-*g*-poly(acrylic acid)/sodium humate superabsorbents. *Polym. Mater. Sci. Eng*. 25: 41–44.

Wang, W.B. and A.Q. Wang. 2009c. Preparation and slow released fertilizer properties of GG-*g*-PAA/SH superabsorbents. *Humic Acid* 1: 19–23.

Wang, W.B. and A.Q. Wang. 2009d. Preparation, characterization and properties of superabsorbent nanocomposites based on natural guar gum and modified rectorite. *Carbohydr. Polym*. 77: 891–897.

Wang, W.B. and A.Q. Wang. 2009e. Synthesis and swelling properties of guar gum-*g*-poly(sodium acrylate)/Na-montmorillonite superabsorbent nanocomposite. *J. Compos. Mater*. 43: 2805–2819.

Wang, W.B. and A.Q. Wang. 2009f. Synthesis, swelling behaviors and slow-release characteristics of guar gum-*g*-poly(sodium acrylate)/sodium humate superabsorbent. *J. Appl. Polym. Sci*. 112: 2102–2111.

Wang, W.B. and A.Q. Wang. 2010a. Adsorption and rheological studies of sodium carboxymethyl cellulose onto kaolin: Effect of degree of substitution. *Carbohydr. Polym.* 82: 83–91.

Wang, W.B. and A.Q. Wang. 2011. Preparation, swelling, and stimuli-responsive characteristics of superabsorbent nanocomposites based on carboxymethyl cellulose and rectorite. *Polym. Adv. Technol*. 22: 1602–1611.

Wang W.B., J. Wang, Y.R. Kang, and A.Q. Wang. 2011e. Synthesis, swelling and responsive properties of a new composite hydrogel based on hydroxyethyl cellulose and medicinal stone. *Composites Part B Eng.* 42: 809–818.

Wang, W.B., J. Wang, and A.Q. Wang. 2012b. pH-responsive nanocomposites from methylcellulose and attapulgite nanorods: Synthesis, swelling and absorption performance on heavy metal ions. *J. Macromol. Sci. Part A* 49: 306–315.

Wang, W.B., J.X. Xu, and A.Q. Wang. 2011f. A pH-, salt- and solvent-responsive carboxymethylcellulose-*g*-poly(sodium acrylate)/medical stone superabsorbent composite with enhanced swelling and responsive properties. *Express Polym. Lett.* 5: 385–400.

Wang, W.B., J.P. Zhang, and A.Q. Wang. 2009b. Preparation and swelling properties of superabsorbent nanocomposites based on natural guar gum and organo-vermiculite. *Appl. Clay Sci.* 46: 21–26.

Wang, W.B., N.H. Zhai, and A.Q. Wang. 2011g. Preparation and swelling characteristics of a superabsorbent nanocomposite based on natural guar gum and cation-modified vermiculite. *J. Appl. Polym. Sci*. 119: 3675–3686.

Wang, W.B., Y.A. Zheng, and A.Q. Wang. 2008b. Syntheses and properties of the superabsorbent composites based on natural guar gum and attapulgite. *Polym. Adv. Technol*. 19: 1852–1859.

Wang, X.H. and A.Q. Wang. 2010b. Adsorption characteristics of chitosan-*g*-poly(acrylic acid)/attapulgite hydrogel composite for Hg(II) ions from aqueous solution. *Sep. Sci. Technol.* 45: 2086–2094.

Wang, X.H. and A.Q. Wang. 2010c. Removal of Cd(II) from aqueous solution by the composite hydrogel based on attapulgite. *Environ. Technol.* 31: 745–753.

Wang, X.H. and A.Q. Wang. 2012. Equilibrium isotherm and mechanism studies of Pb(II) and Cd(II) ions onto hydrogel composite based on vermiculite. *Des. Water Treat.* 48: 38–49.

Wang, X.H., Y.T. Xie, and A.Q. Wang. 2010f. Adsorption behaviors of copper ion(II) on chitosan-*g*-poly(acrylic acid)/vermiculite composites. *China Mining Mag.* 19: 101–104.

Wang, X.H., Y.A. Zheng, and A.Q. Wang. 2009c. Fast removal of copper ions from aqueous solution by chitosan-*g*-poly(acrylic acid)/attapulgite composites. *J. Hazard. Mater.* 168: 970–977.

Wang, X.Y., Y.M. Du, J.W. Luo, B.F. Lin, and J. F. Kennedy. 2007. Chitosan/organic rectorite nanocomposite films: Structure, characteristic and drug delivery behavior. *Carbohydr. Polym.* 69: 41–49.

Wang, X.Y., B. Liu, J.L. Ren, C.F. Liu, X.H. Wang, J. Wu, and R.C. Sun. 2010g. Preparation and characterization of new quaternized carboxymethyl chitosan/rectorite nanocomposite. *Composited Sci. Technol.* 70: 1161–1167.

Wang, X.Y., S.P. Strand, Y.M. Du, and M. Kjell. 2010h. Chitosan–DNA–rectorite nanocomposites: Effect of chitosan chain length and glycosylation. *Carbohydr. Polym.* 79: 590–596.

Wang, Y.Z., X.N. Shi, W.B. Wang, and A.Q. Wang. 2013a. Ethanol-assisted dispersion of attapulgite and its effect on improving properties of alginate-based superabsorbent nanocomposite. *J. Appl. Polym. Sci.* 129: 1080–1088.

Wang, Y.Z., W.B. Wang, X.N. Shi, and A.Q. Wang. 2013b. Enhanced swelling and responsive properties of an alginate-based superabsorbent hydrogel by sodium *p*-styrenesulfonate and attapulgite nanorods. *Polym. Bull.* 70: 1181–1193.

Wu, D., B. Zhang, C. Li, Z. Zhang, and H. Kong. 2006. Simultaneous removal of ammonium and phosphate by zeolite synthesized from fly ash as influenced by salt treatment. *J. Colloid Interface Sci.* 304: 300–306.

Wu, J.H., J.M. Lin, M. Zhou, and C.R. Wei. 2000. Synthesis and properties of starch-graft-polyacrylamide/clay superabsorbent composite. *Macromol. Rapid Commun.* 21: 1032–1034.

Xie, Y.T. and A.Q. Wang. 2009a. Effects of modified vermiculite on water absorbency and swelling behavior of chitosan-g-poly(acrylic acid)/vermiculite superabsorbent composite. *J. Compos. Mater.* 43: 2401–2417.

Xie, Y.T. and A.Q. Wang. 2009b. Preparation and properties of chitosan-g-poly(acrylic acid)/sepiolite superabsorbent composites. *Polym. Mater. Sci. Eng.* 25: 129–132.

Xie, Y.T. and A.Q. Wang. 2009c. Synthesis, characterization and performance of chitosan-g-poly (acrylic acid)/vermiculite superabsorbent composites. *J. Polym. Res.* 16: 143–150.

Xie, Y.T. and A.Q. Wang. 2010. Preparation and swelling behaviour of cts-*g*-poly(acrylic acid)/muscovite superabsorbent composites. *Iran. Polym. J.* 19: 131–141.

Xie, Y.T., A.Q. Wang, and G. Liu. 2010. Effects of modified sepiolite on water absorbency and swelling behavior of chitosan-*g*-poly (acrylic acid)/sepiolite superabsorbent composite. *Polym. Composit.* 31: 89–96.

Xu, J.X., J.P. Zhang, Q. Wang, and A.Q. Wang. 2011. Disaggregation of palygorskite crystal bundles via high-pressure homogenization. *Appl. Clay Sci.* 54: 118–123.

Xu, R.F., S.J. Xin, X. Zhou, W. Li, F. Cao, X.Y. Feng, and H.B. Deng. 2012. Quaternized chitosan–organic rectorite intercalated composites based nanoparticles for protein controlled release. *Int. J. Pharm.* 438: 258–265.

Yan, L., Q. Shuai, X. Gong, Q. Gu, and H. Yu. 2009. Metallic iron filters for universal access to safe drinking water. *Clean-Soil Air Water* 37: 392–397.

Yang, H.X., S.B. Hua, W.B. Wang, and A.Q. Wang. 2011. Composite hydrogel beads based on chitosan and laponite: Preparation, swelling, and drug release behavior. *Iran. Polym. J.* 20: 479–490.

Yang, H.X., W.B. Wang, and A.Q. Wang. 2012. A pH-sensitive biopolymer-based superabsorbent nanocomposite from sodium alginate and attapulgite: Synthesis, characterization and swelling behaviors. *J. Dispersion Sci. Technol.* 33: 1154–1162.

Yang, H.X., W.B. Wang, J.P. Zhang, and A.Q. Wang. 2013. Preparation, characterization and drug-release behaviors of a pH-sensitive composite hydrogel bead based on guar gum, attapulgite and sodium alginate. *Int. J. Polym. Mater.* 62: 369–376.

Yao, S., J. Li, and Z. Shi. 2009. Phosphate ion removal from aqueous solution using an iron oxide-coated fly ash adsorbent. *Adsorpt. Sci. Technol.* 27: 603–608.

Yuan, L. and T. Kusuda. 2005. Adsorption of ammonium and nitrate ions by poly(*N*-isopropylacrylamide) gel and poly(*N*-isopropylacrylamide-*co*-chlorophyllin) gel in different states. *J. Appl. Polym. Sci*. 96: 2367–2372.

Zeng, L., X. Li, and J. Liu. 2004. Adsorptive removal of phosphate from aqueous solutions using iron oxide tailings. *Water Res*. 38: 1318–1326.

Zhang, J., K.H. Lee, L. Cui, and T. Jeong. 2009. Formation of organic nanoparticles by freeze-drying and their controlled release. *J. Ind. Eng. Chem*. 15: 185–189.

Zhang, J., W.Q. Wang, Y.P. Wang, J.Y. Zeng, S.T. Zhang, Z.Q. Lei, and X.T. Zhao. 2007c. Preparation and characterization of montmorillonite/carrageen/guar gum gel spherical beads. *Polym. Polym. Compos.* 15: 131–136.

Zhang, J.P., Y.L. Jin, and A.Q. Wang. 2011. Rapid removal of Pb(II) from aqueous solution by chitosan-*g*-poly(acrylic acid)/attapulgite/sodium humate composite hydrogels. *Environ Technol.* 32: 523–531.

Zhang, J.P., A. Li, and A.Q. Wang. 2005. Swelling behaviors and application of poly(acrylic acid-*co*-acrylamide)/sodium humate/attapulgite superabsorbent composite. *Polym. Adv. Technol.* 16: 813–820.

Zhang, J.P., A. Li, and A.Q. Wang. 2006. Study on superabsorbent composite. VI. Preparation, characterization and swelling behaviors of starch phosphate-graft-acrylamide/attapulgite superabsorbent composite. *Carbohydr. Polym*. 65: 150–158.

Zhang, J.P. and A.Q. Wang. 2010. Adsorption of Pb(II) from aqueous solution by chitosan-*g*-poly(acrylic acid)/attapulgite/sodium humate composite hydrogels. *J. Chem. Eng. Data* 55: 2379–2384.

Zhang, J.P., L. Wang, and A.Q. Wang. 2007a. Preparation and properties of chitosan-*g*-poly(acrylic acid)/montmorillonite superabsorbent nanocomposite via in situ intercalative polymerization. *Ind. Eng. Chem. Res*. 46: 2497–2502.

Zhang, J.P., Q. Wang, and A.Q. Wang. 2007b. Synthesis and characterization of chitosan-*g*-poly(acrylic acid)/attapulgite superabsorbent composites. *Carbohydr. Polym.* 68: 367–374.

Zhang, J.P., Q. Wang, and A.Q. Wang. 2010a. In situ generation of sodium alginate/hydroxyapatite nanocomposite beads as drug controlled release matrices. *Acta Biomater.* 6: 445–454.

Zhang, J.P., Q. Wang, X.L. Xie, X. Li, and A.Q. Wang. 2010b. Preparation and swelling properties of pH-sensitive sodium alginate/layered double hydroxides hybrid beads for controlled release of diclofenac sodium. *J. Biomed. Mater. Res. B* 92B: 205–214.

Zheng, Y.A., S.B. Hua, and A.Q. Wang. 2010. Adsorption behavior of Cu^{2+} from aqueous solutions onto starch-*g*-poly(acrylic acid)/sodium humate hydrogels. *Desalination* 263: 170–175.

Zheng, Y.A., P. Li, and J.P. Zhang. 2007. Synthesis, characterization and swelling behaviors of poly(sodium acrylate)/vermiculite superabsorbent composites. *Eur. Polym. J*. 43: 1691–1698.

Zheng, Y.A. and A.Q. Wang. 2009. Evaluation of ammonium removal using a chitosan-*g*-poly (acrylic acid)/rectorite hydrogel composite. *J. Hazard. Mater.* 171: 671–677.

Zheng, Y.A. and A.Q. Wang. 2010a. Nitrate adsorption using poly(dimethyl diallyl ammonium chloride)/polyacrylamide hydrogel. *J. Chem. Eng. Data.* 55: 3494–3500.

Zheng, Y.A. and A.Q. Wang. 2010b. Potential of phosphate removal using Al^{3+}-crosslinking chitosan-*g*-poly(acrylic acid)/vermiculite ionic hybrid. *Adsorpt. Sci. Technol.* 28: 89–99.

Zheng, Y.A. and A.Q. Wang. 2010c. Enhanced adsorption of ammonium using hydrogel composites based on chitosan and halloysite. *J. Macromol. Sci. Part A Pure Appl. Chem.* 47: 33–38.

Zheng, Y.A. and A.Q. Wang. 2012. Granular hydrogel initiated by Fenton reagent and their performance on Cu(II) and Ni(II) removal. *Chem. Eng. J.* 200: 601–610.

Zheng, Y.A., Y.T. Xie, and A.Q. Wang. 2009a. Adsorption of Pb^{2+} onto chitosan-grafted-poly (acrylic acid)/sepiolite composite. *Environ. Sci*. 30: 2575–2579.

Zheng, Y.A., Y.T. Xie, and A.Q. Wang. 2012. Rapid and wide pH-independent ammonium-nitrogen removal using a composite hydrogel with three-dimensional networks. *Chem. Eng. J*. 179: 90–98.

Zheng, Y.A., J.P. Zhang, and A.Q. Wang. 2009b. Fast removal of ammonium-nitrogen from aqueous solution using chitosan-*g*-poly (acrylic acid)/attapulgite composite. *Chem. Eng. J.* 155: 215–222.